

JGR Biogeosciences



RESEARCH ARTICLE

10.1029/2022JG007084

Key Points:

- Concentration-discharge relationships for different constituents show marked variability among streams from different watersheds
- Total suspended solids, particulate organic carbon, and to a lesser degree, dissolved organic carbon exhibit transport limitation
- The magnitude and composition of constituent fluxes display variability at distinct time scales that affect their transport to the ocean

Supporting Information:

Supporting Information may be found in the online version of this article.

Correspondence to:

M. A. Goñi, miguel.goni@oregonstate.edu

Citation:

Goñi, M. A., Welch, K. A., Ghazi, L., Pett-Ridge, J. C., & Haley, B. A. (2023). Mobilization and export of particulate and dissolved solids and organic carbon from contrasting mountainous river watersheds in California and Oregon. *Journal of Geophysical Research: Biogeosciences*, 128, e2022JG007084. https://doi.org/10.1029/2022JG007084

Received 7 JUL 2022 Accepted 17 MAR 2023

Author Contributions:

Conceptualization: Miguel A. Goñi, Julie C. Pett-Ridge Data curation: Miguel A. Goñi, Kylie A. Welch, Layla Ghazi, Julie C. Pett-Ridge Formal analysis: Kylie A. Welch, Julie C. Pett-Ridge, Brian A. Haley Funding acquisition: Miguel A. Goñi, Julie C. Pett-Ridge, Brian A. Haley Investigation: Miguel A. Goñi, Layla Ghazi, Julie C. Pett-Ridge, Brian A. Haley

© 2023. The Authors.

This is an open access article under the terms of the Creative Commons Attribution License, which permits use, distribution and reproduction in any medium, provided the original work is properly cited.

Mobilization and Export of Particulate and Dissolved Solids and Organic Carbon From Contrasting Mountainous River Watersheds in California and Oregon

Miguel A. Goñi¹, Kylie A. Welch¹, Layla Ghazi¹, Julie C. Pett-Ridge², and Brian A. Haley¹

¹College of Earth, Ocean & Atmospheric Sciences, Oregon State University, Corvallis, OR, USA, ²Department of Crop and Soil Science, College of Agricultural Sciences, Oregon State University, Corvallis, OR, USA

Abstract Concentration-discharge (C-Q) relationships of total suspended solids (TSS), total dissolved solids (TDS), particulate organic carbon (POC), and dissolved organic carbon (DOC) were investigated in the tributaries and main-stems of two mountainous river systems with distinct watershed characteristics (Eel and Umpqua rivers) in Northern California and central Oregon (USA). Power-law ($C = a \times Q^b$) fits to the data showed strong transport-limited behavior (b > 1) by TSS and POC, moderate transport limitation of DOC (b > 0.3) and chemostatic behavior (b < 0) by TDS in most streams. These contrasts led to significant compositional differences at varying discharge levels, with particle-bound constituents becoming increasingly important (relative abundances of 50% to >90%) at high-flow conditions. Organic carbon contents of TSS displayed marked decreases with discharge whereas they increased in TDS during high-flow conditions. Daily and cumulative material fluxes for different coastal streams were calculated using the C-Q relationships and showed that the delivery of transport-limited constituents, such as TSS and POC (and DOC to a lesser degree), was closely tied to high-discharge events and occurred primarily during the winter season. The coherence between winter fluxes and high wave-southerly wind conditions along the coast highlights how seasonal and inter-annual differences in fluvial discharge patterns affect the fate of land-derived materials delivered to coastal regions.

Plain Language Summary Rivers play a key role in transporting materials from land to the ocean. In this study, we investigated several streams of different characteristics from two basins, the Eel River in Northern California and the Umpqua River in central Oregon. We measured how the concentrations of dissolved and particulate materials, including total suspended and dissolved solids and particulate and dissolved organic carbon, varied as a function of river flow. Our results show that different streams export these materials in different ways depending on the level of river flow and certain watershed characteristics. The different trends with river flow exhibited by these constituents impact the total amounts exported by rivers each year as well as the timing of their export. The latter is important because ocean conditions off the Eel and Umpqua rivers exhibit marked contrasts in winds, currents, and waves depending on the season. In the paper, we explore how the combination of the timing of export by the river and the ocean conditions offshore influences the distribution and cycling of particulate and dissolved materials from land in the coastal ocean.

1. Introduction

The magnitude, composition, and timing of dissolved and particulate fluxes by rivers are important variables in the biogeochemical cycles of many elements (e.g., carbon, nitrogen, silica, trace metals) along the land-ocean continuum, from soils and streams to estuaries and the coastal ocean (e.g., Anderson et al., 2019; Drake et al., 2018; Malara et al., 2020; Ward et al., 2017). The transport of particulate and dissolved constituents by streams worldwide reflect a variety of physical, chemical, and biologic processes in watersheds (e.g., Cole et al., 2007; Milliman & Farnsworth, 2013; Raymond et al., 2016; Syvitski et al., 2003). Factors controlling these fluxes and compositions depend on a range of catchment characteristics including climatic variables that regulate hydrologic processes (e.g., infiltration, runoff, hydraulic connectivity), biogeochemical processes that affect their production, retention, and degradation (e.g., productivity, respiration, chemical weathering) as well as geologic and geomorphic variables (e.g., bedrock type, elevation, uplift, landscape type) that control physical weathering, denudation, and erosion. Human-induced changes in watersheds (e.g., dam construction, urbaniza-

GOÑI ET AL. 1 of 30



Journal of Geophysical Research: Biogeosciences

10.1029/2022JG007084

Methodology: Miguel A. Goñi, Layla Ghazi, Julie C. Pett-Ridge, Brian A. Haley

Project Administration: Miguel A. Goñi, Julie C. Pett-Ridge, Brian A. Haley Software: Miguel A. Goñi Supervision: Miguel A. Goñi, Julie C. Pett-Ridge

Visualization: Layla Ghazi Writing – original draft: Miguel A.

Writing – review & editing: Kylie A. Welch, Layla Ghazi, Julie C. Pett-Ridge, Brian A. Halev tion, agriculture, road building, and logging) can impact all these processes and, thus influence the transport of dissolved and particulate constituents by rivers (e.g., Kaushal et al., 2018; Syvitski & Kettner, 2011).

One approach to evaluate the processes controlling the export of different constituents from terrestrial watersheds is to examine the relationships between their concentration and discharge in streams (e.g., Clark et al., 2022; Cohn et al., 1989; Godsey et al., 2009, 2019; Moatar et al., 2017; Syvitski et al., 2000). Thus, for example, constituents that display relative constant (or "flat") concentrations over a broad range of discharge levels are classified as having chemostatic behavior, whereas those that either increase or decrease significantly as discharge changes are classified as displaying ("up" or "down") chemodynamic behavior (Moatar et al., 2017). Chemostatic behavior is often associated with constituents that have relative homogenous distributions and/or production/release rates throughout watersheds (e.g., Thompson et al., 2011), so that changes in flow paths and hydrological connectivity associated with changes in precipitation and runoff do not affect overall constituent concentrations (e.g., Godsey et al., 2009; Mulsoff et al., 2015). In contrast, constituents that display positive ("up") chemodynamic behavior (Moatar et al., 2017) are described as being transport limited, meaning that their distributions and/or production/release rates throughout watersheds are such that their concentrations increase as flows increase. Negative ("down") chemodynamic behavior is characteristic of constituents described as being source limited because their distribution and/or production rates in watersheds is such that their concentrations in stream waters decrease (i.e., are diluted) as flows increase (e.g., Basu et al., 2011; Shanley et al., 2011). Notably, concentration-discharge (C-Q) relationships can be assessed from individual observations at different timescales (e.g., event, inter-annual), as well as from long-term means. Each of these approaches provide different insights into the drivers and controls that affect the mobilization of materials from watersheds (Godsey et al., 2019).

Small mountainous rivers, defined as those with drainage areas <10,000 km² (Milliman & Syvitski, 1992), are important contributors to transport of land-derived materials to the ocean at both regional and global scales (e.g., Bao et al., 2015; Goldsmith et al., 2015; Goñi et al., 2013; Lloret et al., 2013; Milliman & Syvitski, 1992). Small mountainous watersheds are susceptible to storm-induced precipitation events dominating water and material transport. Furthermore, small mountainous rivers are characterized by short channels and small estuaries, which lead to more direct transport to the coastal ocean relative to larger fluvial systems. Because of their rapid hydrologic response, materials transported during flood conditions by small mountainous rivers are delivered to the coastal ocean often under the same dynamic conditions (e.g., storm-induced winds and waves) that lead to high precipitation and elevated fluvial discharges (e.g., Geyer et al., 2000; Kniskern et al., 2011; Wheatcroft, 2000). The coherence between fluvial and coastal oceanic processes directly impacts the distribution and ultimate fate of land-derived materials exported by small mountainous river systems (e.g., Goñi et al., 2021; Hastings et al., 2012; Henderix Freitas et al., 2018; Walsh & Nittrouer, 2009).

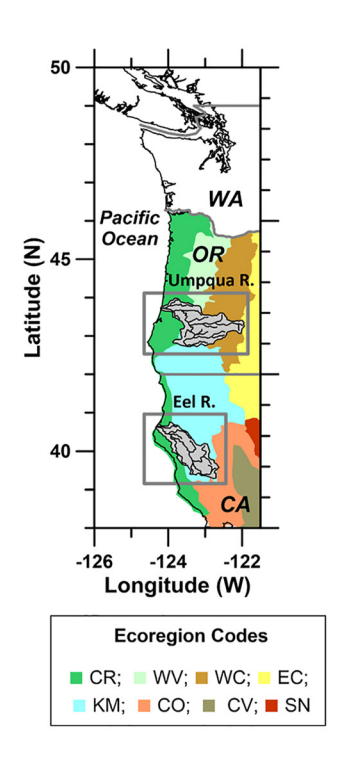
In this study, we seek to evaluate the C-Q relationships of total suspended solids (TSS), total dissolved solids (TDS), particulate organic carbon (POC), and dissolved organic carbon (DOC) in the tributaries and main-stems of two mountainous river systems, the Eel and Umpqua rivers, located along coastal margins of Northern California and central Oregon (USA). The Eel and Umpqua watersheds share some important characteristics, including comparable climate, vegetation, watershed size, mean annual discharge, and landscape uses. However, the two systems also differ greatly in the type of underlying bedrock, soil thickness, and tectonic setting. Because of the flood-dominated nature of these coastal watersheds, our focus is to determine C-Q relationships at event scales for different constituents among the different streams and investigate the compositional differences that occur as function of discharge in the context of watershed characteristics. Furthermore, using these C-Q relationships, we evaluate the timing and magnitude of TSS, TDS, POC, and DOC export fluxes, including their relationship to seasonal ocean conditions offshore (e.g., waves and wind). These findings provide insights into how seasonal and inter-annual differences in fluvial discharge patterns and compositions can affect the fate of land-derived materials entering coastal regions along the west coast of the U.S. (e.g., Hastings et al., 2012; Wheatcroft et al., 2013; Wheatcroft & Sommerfield, 2005), as well as other comparable coastal margins worldwide (e.g., Bright et al., 2020; Clark et al., 2022; Hood et al., 2020; Lin et al., 2020; Reddy et al., 2019).

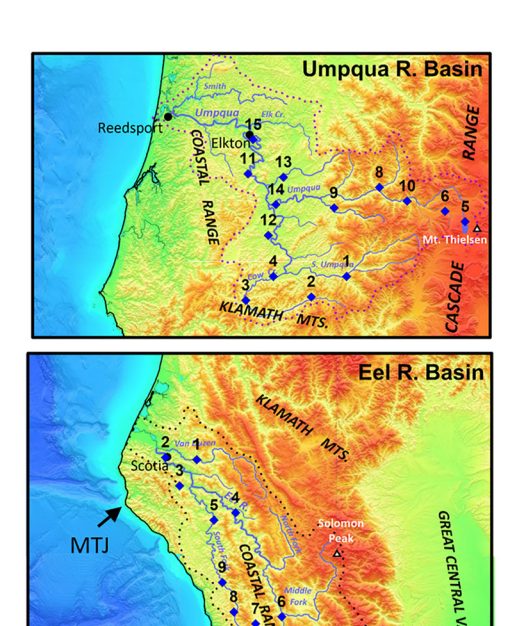
2. Materials and Methods

2.1. Study Area

The work presented here focuses on the Eel and Umpqua river basins, two mountain river systems along the Pacific Northwest margin of the U.S. (Figure 1) that have been the subject of previous studies (see Goñi et al., 2013;

GOÑI ET AL. 2 of 30





Umpqua River

- Stn # USGS Gage Name
- South Umpqua at Tiller
- 2 Cow Creek near Azalea
- 3 West Fork Cow Creek near Glendale
- Cow Creek near Riddle
- 5 Lake Creek near Diamond Lake
- 6 Clear Water River above Trap Creek
- 8 Steamboat Creek near Glide
- 9 Little River at Peel
- 10 North Umpqua W Copelad
- 11 Little Wolf Creek
- 12 Lookinglass Creek at Bockway
- 13 Calapooya Creek near Oakland
- 14 North Umpqua at Winchester
- 15 Umpqua River near Elkton

Eel River

- St # USGS Gage Name
- L Van Duzen near Bridgeville
- Eel River at Scotia
- 3 Bull Creek near Weott
- 4 Eel River at Fort Seward
- 5 South Fork Eel near Miranda
- 6 Middle Fork Eel Near Dos Rios
- 7 Cahto Creek near Laytonville
- 8 Elder Creek near Branscomb
- South Fork Eel at Leggett

Figure 1. Regional and topographic maps of Eel and Umpqua watersheds with locations of USGS gauges sampled during this study. Ecoregion codes are based on Omernik (1987): CR, Coastal Range; WV, Willamette Valley; WC, West Cascades; EC, East Cascades; KM, Klamath Mountains; CO, California Chaparral and Oak Woodland; CV, California Central Valley, SN, Sierra Nevada. MTJ, Mendocino Triple Junction (Clarke, 1992).

Elevation (m)

Ghazi et al., 2022 and references therein). For this project, we collected samples from several USGS gage stations located in different regions of the two river basins with drainage areas that display a number of similarities and contrasts. Ghazi et al. (2022) provide detailed characterization of each watershed and Table 1 summarizes their geology, drainage area, average basin slope, mean annual precipitation, mean runoff, and estimated erosion rate of the main sampling sites. Among the Eel and Umpqua gages sampled, we selected stations with a wide range of drainage areas (10–10,000 km²). Most of the sites have relative steep average basin slopes (15°–25°) characteristic of mountainous river systems. All sites have moderately high levels of annual precipitation with the Eel River sites showing slightly higher values for mean annual precipitation (156 cm) and mean annual runoff (808 mm) rates than the Umpqua River sites (130 cm and 689 mm, respectively). Sedimentary rocks predominate sites from the Eel system whereas in the case of the Umpqua system, several sites drain sedimentary rocks as well as Cascade and Klamath Mountain terranes composed of volcanic and metamorphic rocks.

Because of its location immediately south of the Mendocino Triple Junction (MTJ), the Eel basin is quite active tectonically (Aalto et al., 1995; Gulick et al., 2002) whereas the Umpqua basin is much less so (e.g., Kelsey et al., 1996). Thus, whereas the Eel basin displays uplift rates that range from 3 to 5 mm yr $^{-1}$, uplift rates in the Umpqua basin range from 0 mm yr $^{-1}$ in Western Cascades to 2.5 mm yr $^{-1}$ along the Coast Range (Kelsey et al., 1996; Mitchell et al., 1994). More recent studies (Willenbring et al., 2013) indicate erosion rates, estimated from 10 Be measurements in quartz grains, range from >0.5 mm yr $^{-1}$ in the northern portion of the Eel Basin, which is closest to the MTJ, to 0.17 mm yr $^{-1}$ in the southern most portions of the basin (Fuller et al., 2009). Similar measurements along the Oregon Coast Range indicate erosion rates in regions within the Umpqua Basin are significantly lower, with values that range from 0.05 to 0.2 mm yr $^{-1}$ (Balco et al., 2013; Bierman et al., 2001; Heimsath et al., 2001; Marshall et al., 2017).

The distinct characteristics of these watersheds contribute to observed contrasts in sediment yield among individual stream systems (Table 1). For example, several studies (e.g., Andrews & Antweiler, 2012; Brown & Ritter, 1971; Kelsey, 1980; Wheatcroft & Sommerfield, 2005) show that average sediment yields estimated for most gage stations along the Eel River system (1,500–3,000 ton km⁻² yr⁻¹) are significantly higher relative to those estimated for the Umpqua River gage stations (200–500 ton km⁻² yr⁻¹; Curtiss, 1975; Karlin, 1980; Wheatcroft & Sommerfield, 2005; Wise & O'Connor, 2016). A notable exception is Elder Creek in the southern

GOÑI ET AL. 3 of 30

21698961, 2023, 4, Downloaded from https://agupubs.onlinelibrary.wiley.com/doi/10.1029/2022/G007084 by Oregon State University, Wiley Online Library on [05/04/2023]. See the Terms and Conditions (https://onlinelibrary.wiley.com/nem

USGS gage name	USGS gage #	Geology	Drainage area (km²)	Average basin slope (°)*	Mean annual precipitation (cm) ^c	Mean runoff (mm/ yr) ^c	Erosion rate (mm/ yr)	Average sediment yield (ton/ km²/yr)	Sampling dates in this study	# Samples in this study
Eel River watershed	<u> </u>									
Eel River at Scotia	11477000	Includes all listed below	8,063	18.4	156	808	0.64ª	3062 ^{d,e}	2008, 2009, 2015, 2017, 2018, 2019	29
Van Duzen near Bridgeville	11478500	Central Belt Franciscan	575	17.5	187	1,315	1.11ª	2848 ^{e-i}	2015, 2017, 2018, 2019	15
Bull Creek near Weott	11476600	Coastal Belt Franciscan	73	17.5	166	1,408	0.52 ^{b,**}	2934 ^j	2017, 2018, 2019	22
Eel River at Fort Seward	11475000	Central Belt Franciscan	5,457	18.2	147	744		2089 ^{e,j}	2015, 2017	2
South Fork Eel near Miranda	11476500	Central Belt Franciscan	1,391	19.5	193	1,169	0.48 ^b	1466 ^{e,f,k}	2015, 2017, 2019	3
Middle Fork Eel near Dos Rios	11473900	Central Belt Franciscan	1,930	18.0	143	707		1867 ^{e,f,j}	2015, 2017, 2018, 2019	4
Cahto Creek near Laytonville	11475610	Central Belt Franciscan	13	14.3	222	1,015**		n.d.	2017, 2018, 2019	3
Elder Creek	11475560	Central Belt Franciscan	17	24.1	254	1,330	0.17°	68 ^j	2017, 2018, 2019	15
South Fork Eel at Leggett	11475800	Central Belt Franciscan	642	19.5	206	1,065	0.29 ^b	n.d.	2015, 2017, 2018	2
Umpqua River wate	rshed									
Umpqua River near Elkton	14321000	Includes all listed below	9,539	17.6	130	689	0.14ª	225 ^{d,l,m,n}	2008, 2009, 2015, 2017, 2019	25
Little Wolf Creek	14320934	Oregon Coast Range	23	21.0	126	932	0.33°	525 ¹	2017, 2019	15
North Umpqua at Winchester	14319500	Mixed Oregon Cascades and Oregon Coast Range	3,481	17.0	150	951	n.m.	236 ¹	2015, 2017	2
Calapooya Creek near Oakland	14320700	Oregon Coast Range	544	14.3	141	738#	n.m.	3551	2017, 2019	2
Cow Creek-Riddle	14310000	Klamath Mountains	1,181	20.6	116	611	n.m.	3321	2015, 2017, 2019	3
West Fork Cow Creek near Glendale	14309500	Klamath Mountains	225	22.0	136	1,005	n.m.	n.d.	2017, 2019	2

^aBalco et al. (2013). ^bWillenbring et al. (2013). ^cFuller et al. (2009). ^dWheatcroft and Sommerfield (2005). ^eBrown and Ritter (1971). ^fAndrews and Antweiler (2012). Ekelsey (1980). hKelsey (1977). Janda and Nolan (1979). Calculation using USGS daily sed data from 4 yr in late 1970s, applied to water data 1961-2004. kUSGS water data report for 1981 (only 1yr data). Curtiss (1975). "Karlin (1980). "Wise and O'Connor (2016). "Calculated from Elkton estimates assuming comparable relationship between erosion rate and sediment yield; *USGS StreamStats; **Extrapolated from nearby location (S. Fork Eel at Leggett); #Extrapolated from nearby location (S. Umpqua at Tiller); n.m., not measured.

> section of the Eel River watershed, which has a very low sediment yield (68 ton km⁻² yr⁻¹). This site is characterized by the lowest erosion rates (0.17 mm yr⁻¹) relative to other sites located further north along the Eel River watershed (0.3–1.1 mm yr⁻¹). The relative low uplift rates that characterize this region of the Eel basin, combined with the land use history of the Elder Creek watershed (which unlike most others has not been logged) likely contribute to these unusual low sediment yields for this Eel River tributary (Willenbring et al., 2013).

> In comparison to the large North American rivers that flow into the Pacific Ocean (e.g., Columbia, Fraser, and Sacramento), the Eel and Umpqua systems have been described as small mountainous rivers (e.g., Goñi et al., 2013; Hastings et al., 2012; Wheatcroft et al., 2013; Wheatcroft & Sommerfield, 2005). This categorization

GOÑI ET AL. 4 of 30 is based primarily on the size of the drainage areas of their main-stem gages (<10,000 km²; Table 1), short main channel lengths (193 and 179 km, respectively) and relatively small estuaries (24 and 26 km², respectively) that account for ~0.2% of the total catchment area. Notably, two recent papers investigating the Northeast Pacific Coastal Rainforest region classified the Umpqua and Eel watersheds as "rain continental", a categorization that describes their pluvial water source (Giesbrecht et al., 2022) and their relative large areas with hydrologic regimes typical of interior ecosystems (Bidlack et al., 2021). However, examination of USGS gage records for rivers along the Pacific Northwest margin (Figures S1 and S2 in Supporting Information S1) shows high degree of correlation between daily discharges of the main-stem gages from the Eel and Umpqua rivers and those of other smaller mountainous rivers along the Northern California and Oregon margins. Furthermore, there is a lack of correlation with the Sacramento and the Columbia rivers, which have the two largest watersheds in the region. Thus, from a hydrologic point of view, the Eel and Umpqua watersheds behave very similarly to those of other smaller mountainous rivers in the region, and the magnitude and timing of their material fluxes (see below) are much more representative of the latter rather than large continental systems.

The fate of materials entering the ocean from coastal streams is largely controlled by their composition (e.g., grain size, chemical make-up) as well as the coherence between periods of high discharge and offshore conditions that control their physical dispersion (e.g., Kniskern et al., 2011; Walsh & Nittrouer, 2009; Wheatcroft et al., 2010). Regarding the latter, the Northern California and central Oregon coastlines are characterized by relatively narrow and deep shelves. Both regions experience marked seasonal contrasts in the magnitude and direction of offshore winds, with spring and summer months being characterized by upwelling-favorable northerly winds whereas southwesterly winds that are downwelling-favorable dominate the fall and winter periods (e.g., Checkley & Barth, 2009). Moreover, offshore wave energy also is highly seasonal along the Eel and Umpqua margins, with elevated wave heights being most prevalent during winter months and often associated with winter storm conditions. The coincidence of winter peaks in river discharge with southerly winds and high waves results in conditions in the coastal ocean that facilitate trapping of fluvial materials (including freshwater, suspended, and dissolved materials) in coastal plumes that are pushed against the shoreline by downwelling favorable winds and transported in a net northerly direction by the prevalent seasonal currents (e.g., Mazzini et al., 2014; Pullen & Allen, 2001; Saldias et al., 2020). The high wave energy during winter leads to particle resuspension at shallow depths and limits the deposition of fine sediments along the near-shore regions of both margins, resulting in the formation of mid-shelf sediment depocenters (e.g., Wheatcroft & Borgeld, 2000; Wheatcroft et al., 2013). Because of its greater wave height climatology, the Umpqua mid-shelf depocenter is located at greater depths (80-100 m) than its Eel counterpart (55-80 m). These depocenters are foci of terrestrial POC burial and efficient organic matter preservation (e.g., Hastings et al., 2012; Leithold & Hope, 1999) illustrating the importance of the coherence between discharge and ocean conditions in dictating the fate of fluvial delivered materials (e.g., Kniskern et al., 2011), including both particulate and dissolved loads (e.g., Goñi et al., 2021; Kieft et al., 2020; Wheatcroft et al., 2010). In this paper, we explore these relationships in the context of the magnitude and composition of fluvial materials exported by both river systems.

2.2. Sample Collection and Handling

All the stream samples were collected at USGS gage stations along both the Eel and Umpqua watersheds (Figure 1). Water samples were collected manually using alpha bottles deployed from bridges (Goñi et al., 2013) and dip bottles in the case of smaller tributaries. In both cases, samples were collected below the surface by submerging the bottles before collecting the sample. After collection, samples were transferred to opaque Nalgene bottles and filtered for analyses either in the field or at mobile lab locations within a few hours of collection. We also used Teledyne ISCO samplers deployed prior and during storm events to collect water samples at higher resolution. We typically collected 1 L samples via the ISCO sampler pump system at pre-determined intervals (typically 1–4 hr) with the intake situated below the surface and adjacent to the USGS gages at selected sites. ISCO samplers were turned around every 24 hr and water samples processed in mobile laboratories immediately after collection. Comparison of samples collected manually and via ISCO samplers revealed comparable concentrations and compositions (see below).

Table 1 includes the number of samples collected at each locations and Table S1 in Supporting Information S1 provides details of their collections dates. As can be seen from these data, several sites were sampled at higher frequency over a broad range of discharges, including the gage stations for the Van Duzen, Eel River at Scotia,

GOÑI ET AL. 5 of 30

21698961, 2023, 4, Download

are governed by the applicable Creative C

Bull Creek, Elder Creek, Little Wolf Creek, and Umpqua River at Elkton. These locations are the focus of the detailed investigations of the *C-Q* relationships presented below, but we present data from all other gages to provide a broader context for the relationships discussed. We note that much of our sampling was focused during the wet seasons, when these streams transport the majority of their particulate and dissolved loads. The mainstem gage stations in both the Eel (Scotia) and the Umpqua (Elkton) had the higher number of samples and included data collected during a prior study (Goñi et al., 2013).

2.3. TSS, TDS, POC, and DOC Analyses

In order to determine TSS concentrations, known volumes of water (100–500 ml) were vacuum-filtered onto pre-combusted (450°C for 3 hr), pre-weighted 47 mm diameter, GF/F filters (0.7 μ m nominal pore size). Once filtered, samples were kept frozen inside individually labeled petri dishes until they were oven dried (60°C for 24 hr). Following the drying step, filters were weighed and the mass of TSS calculated by subtracting the weight of the filter. TSS concentrations (g m⁻³) were calculated by dividing the mass of TSS by the volume filtered.

TDS concentrations were determined by filtering known volumes of water (\sim 250 ml) through 0.8 µm polyether-sulfone membrane filters to remove particulate materials. We used this pore size cutoff to be able to compare TDS and TSS concentrations directly. Filtered water samples were split for major cations and anions determinations. Analytical details on these determinations are provided by Ghazi et al. (2022), who also found no difference in TDS concentrations between samples filtered at 0.2 and 0.8 µm filters. Briefly, concentrations of anions (Cl⁻, NO₃⁻, PO₄³⁻, F⁻ and SO₄²⁻) were determined using a Dionex 1500 Ion Chromatograph using the US EPA Method 9056A. Major cations (including Al, B, Ba, Ca, Fe, K, Li, Na, Mg, S, Si, and Sr) were measured with a Spectros Arcos ICP-OES in axial mode at the Keck Collaboratory at Oregon State University. Separate aliquots of the filtered sample were collected in 350 ml amber glass bottles with crimp-sealed polyurethane lined metal caps, preserved with ~30 µmol HgCl₂ for TCO₂ and pCO₂ analysis. These two parameters were then used to solve for the other carbonate system parameters, including HCO₃ concentrations (Bandstra et al., 2006).

Based on previous studies (e.g., Gaillardet et al., 1999), we determined TDS concentrations by summing the concentrations of the following major ions, HCO_3 , SiO_2 , SO_4 *, Na*, Mg*, Ca*, K*, where * indicates concentrations corrected for atmospheric inputs following the procedure outlined by Ghazi et al. (2022). To be consistent with the TSS and POC determinations (see below), we added the concentration of dissolved organic matter (DOM), which was estimated by assuming DOM is 50% DOC (see below) by weight (e.g., Thurman, 1985; p. 12). Thus, TDS concentrations (g m⁻³) in this study are calculated as TDS = $HCO_3 + SiO_2 + SO_4 * + Na^* + Mg^* + Ca^* + K^* + 2 \times DOC$.

POC concentrations were determined by filtering known volumes (50–100 ml) of water through 13 mm diameter GF/F filters (0.7 μ m nominal pore size). Once filtered, samples were exposed to concentrated HCl acid fumes to remove carbonates and then analyzed by high-temperature combustion according to established procedures using a Costech ECS 4010 CN analyzer (e.g., Goñi et al., 2019). POC concentrations (g m⁻³) were calculated by dividing the mass of carbon by the volume filtered. In the case of DOC, water samples were filtered through 0.45 μ m pore-sized acro-discs immediately after collection, into pre-acidified amber glass vials. We realize the pore size of the DOC membranes is slightly different than the ones used for other constituents (e.g., TDS). These differences reflect operational definitions based on available membranes and established methodology (e.g., Thurman, 1985). We measured DOC concentrations (g m⁻³) by high-temperature oxidation using a Shimadzu TOC-VSCH analyzer at the Oregon State University's Institute for Water and Watersheds Collaboratory.

2.4. River Discharge Data

River discharge data (Q; m³ s⁻¹) were acquired from USGS gage records at each of the stations sampled. Instantaneous discharge measurements at time of each sample collection were used to investigate C-Q relationships using the same approach as Ghazi et al. (2022). We used the USGS daily discharge data to investigate seasonal and inter-annual variability in discharge and fluxes for water years 2016 (1 October 2015 to 30 September 2016), 2017 (1 October 2016 to 30 September 2017), 2018 (1 October 2017 to 30 September 2018) and 2019 (1 October 2018 to 30 September 2019).

2.5. Offshore Wave and Wind Data

To investigate conditions in the coastal ocean regions adjacent to the two study areas, we used wave height and wind speed and direction data from National Data Buoy Center buoys located offshore (~400 m water depth)

GOÑI ET AL. 6 of 30

21698961, 2023, 4, Download

along the Northern California (Station 46022, 40°44'53" N 124°31'37" W) and central Oregon (Station 46050, 44°40'8" N 124°32'46" W) margins. All the offshore data were available in 15 min intervals and we calculated daily averages to match the temporal resolution of the USGS daily discharge data. In the case of the offshore wind data, we calculated the north-south wind velocity vectors to illustrate upwelling-favorable (winds from the north) versus downwelling-favorable (winds from the south) conditions.

2.6. Concentration-Discharge (C-Q) Relationships and Material Fluxes

We examined the relationships between TSS, TDS, POC, and DOC concentrations and Q by plotting them in log-log space and deriving a power-law statistical fit (Equation 1):

$$C_i (g m^{-3}) = a_i \times Q (m^3 s^{-1})^{bi}$$
 (1)

where C_i represents concentration of constituent i, Q is discharge, and a_i and b_i represent the power-fit parameters for each constituent. We used the RStudio stats package; https://www.R-project.org/) to calculate the p-values for the power law C-Q fits and the 95% confidence interval (95% c.i.) for the intercepts and slopes of the C-Q relationships. The approach to examine C-Q relationships used here is a simplified version of the "quasi-maximum likelihood estimator" method described by Cohn et al. (1992) to calculate rating curves (e.g., Goñi et al., 2013; Syvitski et al., 2000). Because particulate loads at very low flows often include autochthonous materials (e.g., river algae) rather than materials mobilized from the watershed, selected samples collected at very low discharges were excluded from C-Q fits (e.g., Hatten et al., 2012; Wheatcroft & Sommerfield, 2005). Power fits were applied to streams with 10 or more samples. Given the relatively small number of observations, the simple regressions presented here should not be considered rating curves for the streams sampled; rather they describe the relationship between discharge and TSS, TDS, POC, and DOC concentrations under a range of discharges. In view of the modest samples sizes, we used the 95% c.i. of each fit parameter to assess differences among streams.

Overall, these relationships can be used to explore biogeochemical and hydrological contrasts (e.g., Clark et al., 2022; Moatar et al., 2017) among streams (e.g., Hood et al., 2020; Lloret et al., 2013) and to investigate relationships between fluvial fluxes and offshore conditions (e.g., Kniskern et al., 2011). In this paper, we applied the approach of Lloret et al. (2013) to calculate TSS, TDS, POC, and DOC fluxes for different streams and evaluate temporal changes in compositions of the dissolved and particulate loads. First, we used the *C-Q* relationships determined from the individual samples to calculate concentrations based on the daily discharge records from USGS gages. We then multiplied the resulting Ci's by the daily discharge to estimate daily fluxes according to Equation 2:

$$F_i(g d^{-1}) = C_i(g m^{-3}) \times Q(m^3 d^{-1}) = a_i \times Q(m^3 d^{-1})^{b_i+1}$$
(2)

where F_i is the daily flux of constituent i, C_i is the concentration determined by the power law fit using the a_i and b_i parameters and Q is the daily discharge. Daily fluxes were added to calculate cumulative fluxes for the 2016, 2017, 2018, and 2019 water years. Because of the relative paucity of data during different seasons, we consider these fluxes to be semi-quantitative, and thus present them as part of the discussion. Nevertheless, they are useful to examine patterns of fluvial export and investigate trends in both the magnitude and timing of different constituent fluxes from different watersheds.

2.7. Particulate and Dissolved Compositional Parameters

The daily TSS, TDS, POC, and DOC concentrations calculated from the C-Q relationships were also used to compute four compositional parameters that describe their relative abundances as a function of discharge. The four parameters calculated from the daily concentration data include the fraction of TSS as a percentage of total dissolved and particulate load (Frac_{TSS} = $100 \times [TSS/(TSS + TDS)]$), the fraction of POC calculated as a percentage of total organic carbon (Frac_{POC} = $100 \times [POC/(POC + DOC)]$), the mass abundance of POC as a percentage of TSS (%POC = $100 \times (POC/TSS)$), and the mass abundance of DOC as a percentage of TDS (%DOC = $100 \times (DOC/TDS)$). These parameters have been used in previous studies to evaluate temporal (seasonal and inter-annual) trends in the compositions of fluvial material export (e.g., Coynel et al., 2006; Moukandi N'akya et al., 2020) and compare the nature and dynamics of suspended and dissolved loads across different river systems (e.g., Laraque et al., 2013). In this paper, we use these parameters to investigate patterns

GOÑI ET AL. 7 of 30

Table 2Concentration (C) Versus Discharge (O) Power Fit Parameters: $\lceil C \rceil = a \times \lceil O \rceil^b$

Parameter	Eel River (Scotia)	Van Duzen (Bridgeville)	Bull Creek (Weott)	Elder Creek (Branscomb)	Umpqua River (Elkton)	Little Wolf Creek
TSS (g m ⁻³)						
a (95% c.i.)	0.0055 (0.0495)	0.43 (0.12)	0.61 (0.27)	1.71 (4.61)	0.032 (0.067)	1.38 (1.88)
b (95% c.i.)	1.62 (0.46)	1.36 (0.46)	2.60 (0.54)	0.93 (1.49)	1.13 (0.40)	1.75 (0.28)
r^2 (p-value)	0.89 (<0.001)	0.93 (<0.001)	0.95 (<0.001)	0.47 (<0.05)	0.85 (<0.001)	0.98 (<0.001)
TDS $(g m^{-3})$						
a (95% c.i.)	231 (20)	192 (14)	141 (5)	88.4 (1.0)	84.4 (12.6)	42.2 (1.1)
b (95% c.i.)	-0.116 (0.070)	-0.159 (0.084)	-0.131 (0.066)	-0.101 (0.045)	-0.070 (0.098)	-0.077 (0.038)
r^2 (p-value)	0.83 (<0.001)	0.85 (<0.001)	0.78 (<0.001)	0.88 (<0.001)	0.54 (<0.01)	0.88 (<0.001)
POC (g m ⁻³)						
a (95% c.i.)	0.00035 (0.051)	0.021 (0.106)	0.051 (0.296)	0.165 (0.338)	0.013 (0.057)	0.071 (0.194)
b (95% c.i.)	1.39 (0.45)	1.08 (0.49)	1.79 (0.50)	0.81 (1.05)	0.78 (0.42)	1.71 (0.72)
r^2 (p-value)	0.87 (<0.001)	0.88 (<0.001)	0.92 (<0.001)	0.47 (<0.01)	0.73 (<0.001)	0.90 (<0.001)
DOC (g m^{-3})						
a (95% c.i.)	0.51 (0.31)	0.81 (0.51)	1.00 (0.47)	1.06 (1.48)	1.62 (3.03)	1.15 (2.15)
b (95% c.i.)	0.31 (0.17)	0.31 (0.15)	0.36 (0.31)	0.35 (0.38)	0.071 (0.163)	0.34 (0.34)
r^2 (p-value)	0.86 (<0.001)	0.86 (<0.001)	0.54 (<0.001)	0.55 (<0.01)	0.55 (<0.01)	0.62 (<0.001)

Note. TSS, total suspended solids; TDS, total dissolved solids; POC, particulate organic carbon; DOC, dissolved organic carbon. Data shown include the calculated value and 95% confidence interval (in italics) for each parameter, correlation coefficient r^2 , and probability (p-value in italics).

in the compositions of the particulate and dissolved loads as a function of discharge conditions among streams with distinct watershed and hydrological characteristics. Furthermore, we present 7-day running averages of these parameters during the 2016, 2017, 2018, and 2019 water years to examine the compositional variability of materials exported by the Eel and Umpqua rivers as a function of offshore conditions (i.e., wind and waves) along the coastal margin.

3. Data

All the concentration data for all the samples collected from the different stream gage stations are tabulated in Table S1 in Supporting Information S1 and archived at the hydroshare archival site (https://www.hydroshare.org; Goni et al., 2022). River discharge data are available through the USGS National Water Information System (https://waterdata.usgs.gov/nwis). All wind and wave data are available through NOAA's National Buoy Data Center portal (https://www.ndbc.noaa.gov/).

4. Results

4.1. Concentration-Discharge Relationships

In the following sections, we describe the concentrations of TSS, TDS, POC, and DOC for the different stream sites in the Eel and Umpqua watersheds in relationship to the instantaneous discharge values at the time of collection. We use log-log plots to illustrate the power relationships between discharge and concentration and summarize the fit parameters for locations where there were enough data (n > 10) to calculate meaningful fits (see Table 2). Figure S3 in Supporting Information S1 illustrates the magnitude and variability (95% c.i.) of the b exponents for the different power relationships among the different streams.

4.1.1. Total Suspended and Dissolved Solids

TSS concentrations in samples collected throughout the Eel River watershed ranged from 0.3 to 3,000 g m⁻³, with significant variability in the TSS-Q relationships among the different streams (Figure 2a). For example, of the four stream gage stations sampled with high enough frequency to calculate a power-law fit, Bull Creek was characterized by the steepest increase with discharge, resulting in the largest exponent ($b_{\text{TSS}} = 2.60$; Table 2).

GOÑI ET AL. 8 of 30

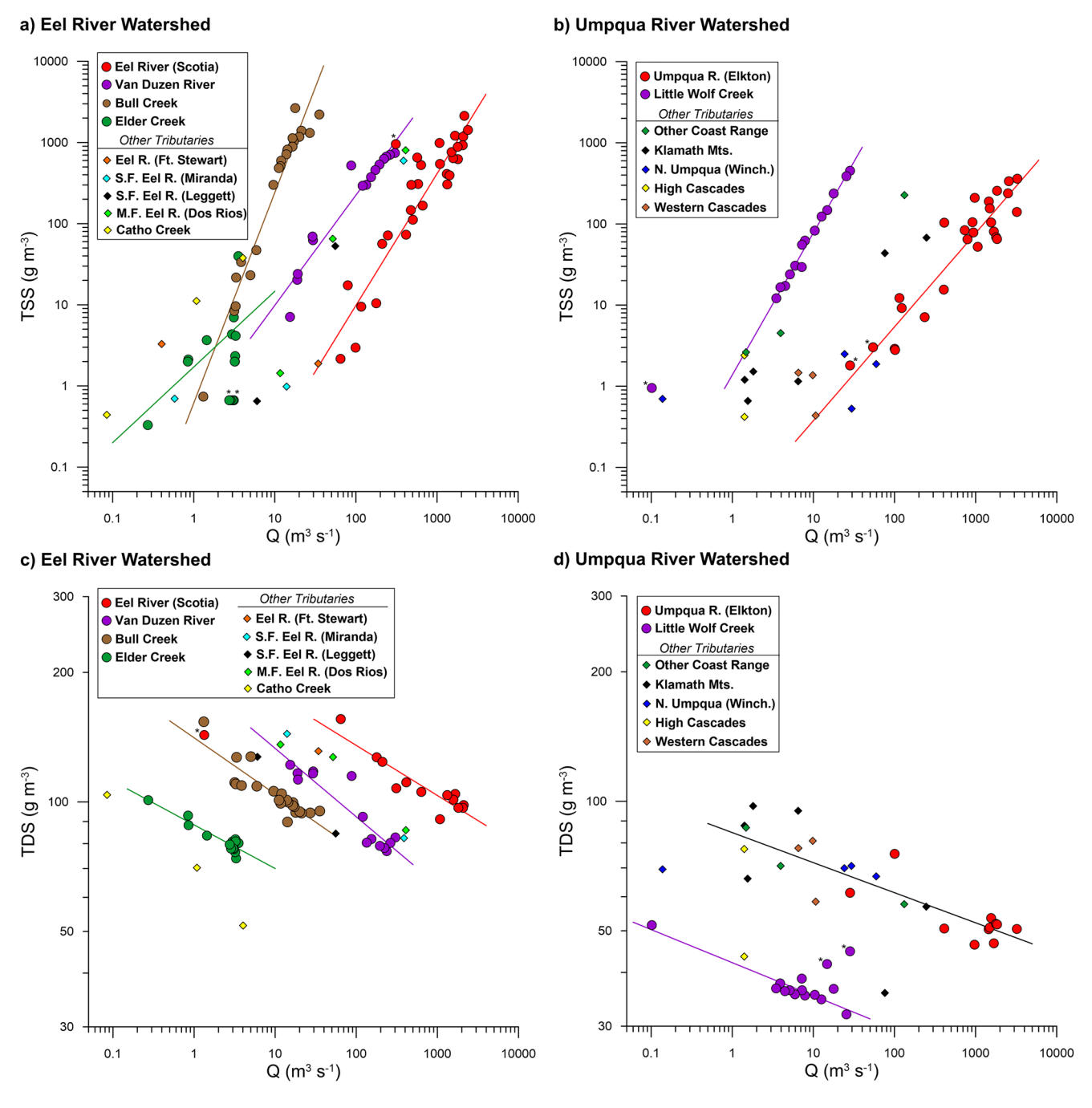


Figure 2. Discharge-concentration relationships for (a) total suspended solids (TSS) in Eel basin streams, (b) TSS in Umpqua basin streams, (c) total dissolved solids (TDS) in Eel basin streams, and (d) TDS in Umpqua basin streams. Lines correspond to power fits for different streams (see Table 2); * indicates data points excluded from power fit calculations (see text).

The main stem of the Eel River at Scotia had the second largest exponent ($b_{\rm TSS}=1.62$) whereas the Van Duzen displayed a somewhat lower exponent for its power fit ($b_{\rm TSS}=1.36$). Elder Creek, which is located in the southern region of the Eel River watershed, displayed much less steep TSS increases with increasing Q ($b_{\rm TSS}=0.93$; Table 2). Less frequent observations from other stream gage stations (e.g., Cahto Creek, South Fork of Eel at Miranda and Leggett, and Middle Fork at Dos Rios) show most other streams display elevated TSS concentrations at high flows (Figure 2a) and are included in this graph for comparison to sites with more frequent measurements.

Among samples from the Umpqua River watershed, TSS concentrations ranged from 0.5 to 500 g m⁻³ and, as in the Eel, displayed positive relationships with discharge (Figure 2b). The maximum TSS concentrations in

GOÑI ET AL. 9 of 30

Umpqua watershed streams were markedly lower than in the Eel counterparts and the trends with discharge showed increases in TSS that were more moderate. Thus, for example, Little Wolf Creek, which is a small-sized system draining the Oregon Coastal range, had the steepest exponent ($b_{\rm TSS}=1.75$; Table 2) for its TSS-Q fit, but it was considerably lower than that of Bull Creek in the Eel system (Figure S3 in Supporting Information S1). Similarly, the main-stem of the Umpqua River at Elkton also displayed a power-law exponent ($b_{\rm TSS}=1.15$) that was lower than that displayed by the main stem of the Eel at Scotia (Table 2). Other gage stations within the Umpqua River systems had TSS-Q relationships that were comparable to those from the Umpqua main stem (Figure 2b).

Total dissolved solid concentrations in samples from the Eel River watershed streams were markedly lower than their respective TSS concentrations and ranged from 50 to 150 g m⁻³ (Figure 2c). Unlike TSS, TDS concentrations showed steady decreases with increased discharge leading to power fits that had negative exponents $(-0.10 \le b_{\text{TDS}} \le -0.16)$ for all four stream gage stations where there were enough data to estimate statistically significant relationships (Table 2). The ranges in concentrations among the four sites were comparable despite differences in discharge and watershed size. Notably, Elder Creek and Cahto Creek, both small watersheds in southern region of the Eel Basin, displayed lower TDS concentrations at base flows relative to the other streams.

TDS concentrations in samples from stream gage stations along the Umpqua River basin ranged from 30 to 100 g m⁻³ and were generally lower than their TSS counterparts, although not to the degree measured in most of the Eel River streams. Similarly to the Eel system, TDS concentrations in the Umpqua watershed displayed decreases with increasing discharge (Figure 2d) albeit the decreases were less steep than for the Eel River streams. These differences resulted in less negative exponents for the TDS-Q power fits (b_{TDS} values of -0.070 and -0.077; Table 2) calculated for the two stream gages in this system with enough observations (Umpqua River at Elkton and Little Wolf Creek, respectively).

4.1.2. Particulate and Dissolved Organic Carbon

POC concentrations in stream waters from the Eel River gage stations ranged from 0.04 to 40 g m⁻³ and, similarly to TSS, displayed strong increases with increasing discharge (Figure 3a). As was the case with TSS, different stream systems had distinct POC-Q relationships. Bull Creek, which has a small-sized watershed located in the northern section of the Eel basin, displayed the steepest increase that resulted in the largest exponent in the power law fit ($b_{POC} = 1.79$; Table 2). The main stem of Eel River at Scotia had the second highest exponent ($b_{POC} = 1.39$), followed by Van Duzen ($b_{POC} = 1.08$). Most other gage stations displayed POC concentrations at specific discharges that were consistent with the trends from these systems. As was the case with TSS, the main exception were the two gage stations from the southern Eel River Basin, Cahto Creek and especially Elder Creek, the latter of which showed considerable variability in the POC-Q relationship and had a smaller exponent for its power-law fit ($b_{POC} = 0.81$; Table 2).

In the Umpqua River system, POC concentrations ranged from 0.06 to 30 g m⁻³ and also increased with increasing discharge (Figure 3b). Notably, POC concentrations in the Umpqua streams were generally lower than those in their Eel counterparts with comparable watershed sizes. At the Umpqua River at Elkton gage station, the increase in POC was less steep than in its Eel River at Scotia main-stem counterpart, resulting in power law fit exponent that was less than 1 ($b_{POC} = 0.78$). In contrast, Little Wolf Creek, which is a small and relative steep watershed in the eastern flank of the Oregon Coast range, displayed a steeper increase in POC concentration and an exponent for its power fit ($b_{POC} = 1.71$; Table 2) that was comparable to that of Bull Creek in the Eel basin (Figure S3 in Supporting Information S1).

DOC concentrations displayed a narrower range (0.3–8 g m⁻³) in both the Eel and Umpqua basin streams (Figures 3c and 3d) and were significantly lower at high discharges relative to POC concentrations (Figures 3a and 3b). In the case of samples from the Eel River system, DOC concentrations displayed moderate increases with increasing discharge (Figure 3c). The steepness of the increase in DOC concentrations was considerably less than for TSS and POC, but unlike TDS, all four gage stations where we had enough observations to yield statistically significant trends displayed comparable positive exponents (0.31 $\leq b_{DOC} \leq$ 0.36; Table 2).

In the case of the Umpqua streams (Figure 3d), the overall ranges in DOC concentrations were similar to those in the Eel sites (Figure 3c) but the increases with discharge were generally minimal. Thus, for example, in the case of the main stem of the Umpqua River at Elkton, the exponent of the power-law fit ($b_{\rm DOC}=0.07$) was markedly lower than for the stream gage stations in the Eel system ($b_{\rm DOC}\sim0.3$; Table 2). On the other hand, Little Wolf Creek displayed a power-law fit exponent ($b_{\rm DOC}=0.34$) that was comparable to those from the streams in the Eel River basin (Table 2; Figure S3 in Supporting Information S1).

GOŇI ET AL. 10 of 30

21698961, 2023, 4, Downloaded from https://agupubs.onlinelibrary.wiley.com/doi/10.1029/2022IG007084 by Oregon State University, Wiley Online Library on [05/04/2023]. See the Terms and Conditions (https://onlinelibrary

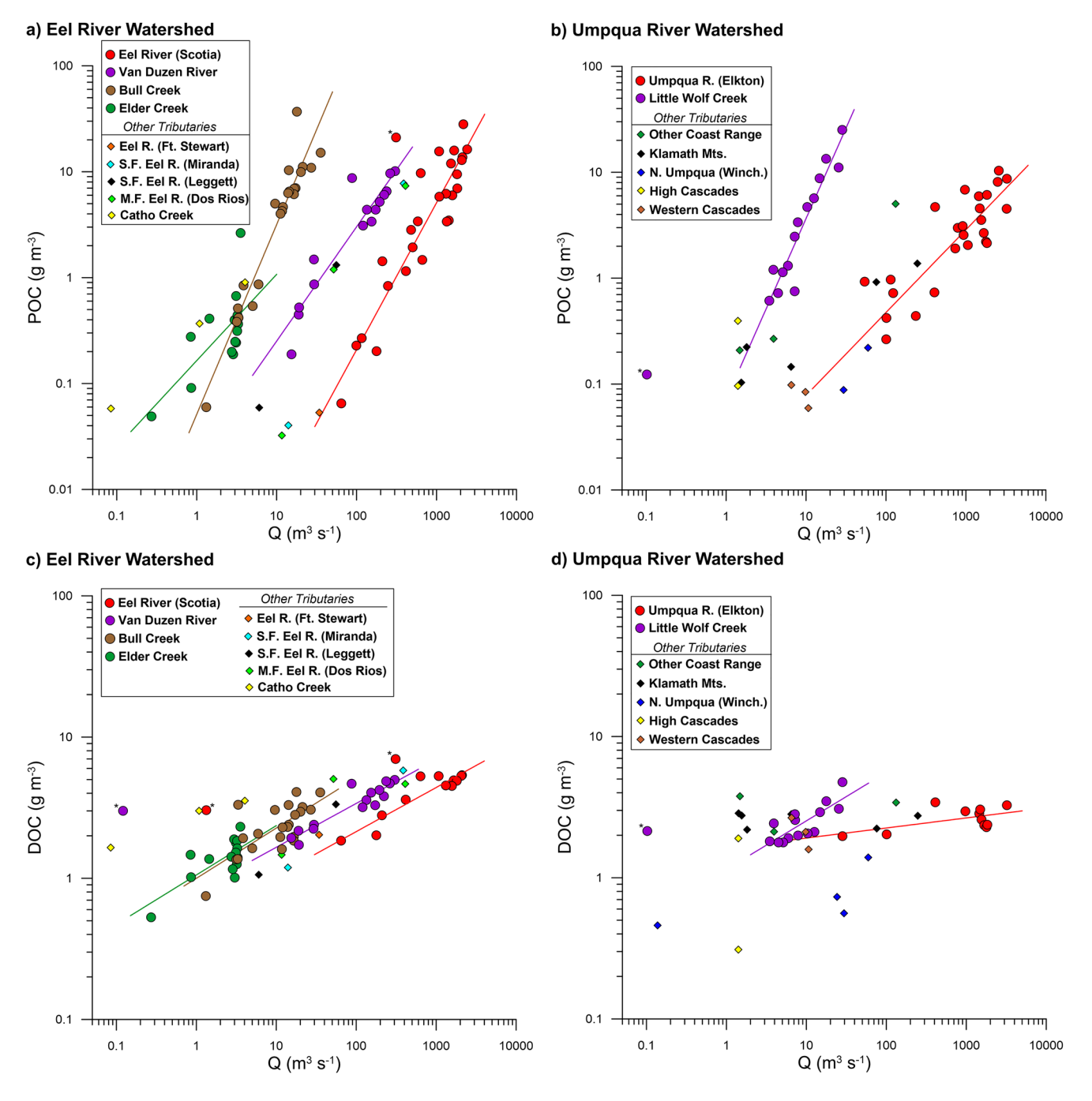


Figure 3. Discharge-concentration relationships for (a) particulate organic carbon (POC) in Eel basin streams, (b) POC in Umpqua basin streams, (c) dissolved organic carbon (DOC) in Eel basin streams, and (d) DOC in Umpqua basin streams. Lines correspond to power fits for different streams (see Table 2); * indicates data points excluded from power fit calculations (see text).

4.2. Compositional Parameters

Previous studies have shown rivers can exhibit marked contrasts in the compositions of their particulate and dissolved loads at different discharge levels and conditions (e.g., Creed et al., 2015; Goñi et al., 2013; Torres et al., 2015), providing insights into the processes that control mobilization of organic materials from different river basins. In this section, we use the concentration data from individual samples to compute four compositional parameters: Frac_{TSS}, Frac_{POC}, %POC, and %DOC, and compare compositions across stream systems with different watershed sizes and discharges. In the following graphs, we chose to plot compositional data as a function of

GOÑI ET AL. 11 of 30

 Table 3

 Compositional Parameters (Average ± Standard Error) for Different Streams at Distinct Discharge Conditions

Parameter	Eel River (Scotia)	Van Duzen (Bridgeville)	Bull Creek (Weott)	Elder Creek (Branscomb)	Umpqua River (Elkton)	Little Wolf Creek
Frac _{TSS} (%)						
$Q:Q_m < 1$	$3\pm 2(n=3)$	$13 \pm 4 \ (n=3)$	$4 \pm 3 \ (n = 2)$	$0.3 \pm \text{n.a.} (n = 1)$	$4 \pm \text{n.a.} (n = 1)$	$2 \pm \text{n.a.} (n = 1)$
$1 < Q:Q_m < 3$	$54 \pm 18 \; (n=3)$	$36\pm 1\ (n=2)$	$28\pm10(n=6)$	$2.9 \pm 0.7 (n = 3)$	$67 \pm \text{n.a.} (n = 1)$	n.m.
$Q:Q_{m} > 3$	$88\pm 2\ (n=8)$	$86 \pm 2 \; (n=10)$	$90 \pm 1 \; (n = 14)$	$4.4 \pm 0.9 \ (n=6)$	$69 \pm 4 \ (n = 8)$	$56 \pm 7 \ (n = 12)$
Frac _{POC} (%)						
$Q:Q_{m} < 1$	$6 \pm 3 \ (n = 2)$	$16 \pm 4 \ (n=3)$	$15 \pm 7 \ (n=2)$	$8 \pm \text{n.a.} (n = 1)$	$12 \pm \text{n.a.} (n = 1)$	$5 \pm \text{n.a.} (n = 1)$
$1 < Q:Q_m < 3$	$44 \pm 16 \ (n = 3)$	$33 \pm 7 \ (n=2)$	$31 \pm 7 \ (n = 6)$	$16 \pm 4 \ (n=3)$	$58 \pm \text{n.a.} (n = 1)$	n.m.
$Q:Q_m > 3$	$66 \pm 3 \ (n = 8)$	$58\pm 2(n=10)$	$75 \pm 2 \ (n = 14)$	$22 \pm 3 \ (n = 11)$	$58 \pm 3 \ (n = 8)$	$54 \pm 6 \ (n = 14)$
%POC (wt.%)						
$Q:Q_{m} < 1$	$3.9 \pm 1.3 \; (n=4)$	$2.3 \pm 0.2 (n = 3)$	$6.3 \pm 1.7 \ (n=2)$	$15 \pm \text{n.a.} (n = 1)$	$14 \pm 4 \ (n = 5)$	$13 \pm \text{n.a.} (n = 1)$
$1 < Q:Q_{\rm m} < 3$	$1.6 \pm 0.2 \; (n=7)$	$1.8 \pm 0.4 (n = 2)$	$2.6 \pm 0.6 (n=6)$	$10 \pm 3 \ (n = 3)$	$5.2 \pm 0.5 \ (n=3)$	n.m.
$Q:Q_m > 3$	$1.2 \pm 0.1 \ (n = 16)$	$1.2 \pm 0.1 \; (n=10)$	$0.85 \pm 0.06 (n=14)$	$20 \pm 3 \ (n = 11)$	$3.2 \pm 0.1 \ (n=17)$	$4.9 \pm 0.3 \; (n=14)$
%DOC (wt.%)						
$Q:Q_{m} < 1$	$1.6 \pm 0.3 \; (n=3)$	$2.1 \pm 0.4 (n = 4)$	$0.86 \pm 0.37 \; (n=2)$	$0.52 \pm \text{n.a.} (n = 1)$	$3.0 \pm 0.3 \; (n=2)$	$4.2 \pm \text{n.a.} (n = 1)$
$1 < Q:Q_{\rm m} < 3$	$4.0 \pm 1.3 \; (n=3)$	$2.0 \pm 0.1 \ (n=2)$	$1.9 \pm 0.3 \; (n=6)$	$1.5 \pm 0.2 \ (n=3)$	$6.8 \pm \text{n.a.} (n = 1)$	n.m.
$Q:Q_m > 3$	$5.1 \pm 0.2 \; (n=8)$	$5.0 \pm 0.3 \; (n=9)$	$2.8 \pm 0.2 (n = 14)$	$2.0 \pm 0.1 \ (n = 11)$	$5.4 \pm 0.3 \ (n = 8)$	$6.8 \pm 0.5 (n = 14)$

Note. $Q:Q_m$, ratio of discharge to mean annual discharge for each stream; Fract_{TSS}, fraction (in %) of total suspended solids relative to the sum of total suspended and dissolved solids; Frac_{POC}, fraction (in %) of particulate organic carbon relative to the sum of particulate and dissolved organic carbon; %POC, weight percent content of particulate organic carbon in total suspended solids; %DOC, weight percent content of dissolved organic carbon in total dissolved solids; n.a., not applicable because there is only one sample for the given range of discharge; n.m., not measured because there are no samples for the given range of discharge.

discharge measurements normalized to the long-term mean discharge of each system $(Q:Q_m)$. Table 3 summarizes average values for the four compositional parameters at different ranges of $Q:Q_m$ for the stream gage stations where multiple samples were collected. Whisker plots of these parameters are shown in Figure S4 in Supporting Information S1 to illustrate statistical variability among the different gage stations and different discharge levels.

4.2.1. Suspended and Dissolved Abundances

The majority of the river sites displayed steep increases in $\operatorname{Frac}_{\operatorname{TSS}}$ with increasing $Q:Q_m$ (Figures 4a and 4b). At base flow levels $(Q:Q_m < 1)$, most samples displayed compositions dominated by TDS and resulted in $\operatorname{Frac}_{\operatorname{TSS}}$ values for both Eel and Umpqua systems of less than 10% (Table 3). The relative importance of the suspended load increased steadily with discharge in most systems, with $\operatorname{Frac}_{\operatorname{TSS}}$ values > 20% at $Q:Q_m \sim 3$. At higher discharges $(Q:Q_m > 3)$, most of the systems showed elevated $\operatorname{Frac}_{\operatorname{TSS}}$ (>50%), with several of the Eel River sites displaying a strong dominance of TSS ($\operatorname{Frac}_{\operatorname{TSS}} \ge 90\%$) under these conditions (Table 3). The main exceptions were the two southernmost stream gage stations, Elder Creek, where $\operatorname{Frac}_{\operatorname{TSS}}$ remained low (<10%) at discharges well above base flows, and Cahto Creek, where $\operatorname{Frac}_{\operatorname{TSS}}$ reached $\sim 45\%$ at $Q:Q_m \sim 10$ (Figure 4a). The Umpqua River stream gage stations sampled also displayed high $\operatorname{Frac}_{\operatorname{TSS}}$ values (>50%) at elevated discharge levels ($Q:Q_m > 10$), but the predominance of TSS in the total material load was less than in the Eel River watershed systems (Figure 4b; Table 3).

In terms of the fraction of total organic carbon load associated with POC, most of the stream systems sampled showed a similar pattern to that of $Frac_{TSS}$, with steep increases in $Frac_{POC}$ as discharge levels increased (Figures 4c and 4d). Similarly to the trends in $Frac_{TSS}$, Bull Creek and Eel River at Scotia displayed the highest $Frac_{POC}$ values (~75%) at $Q:Q_m > 3$, with the Van Duzen also displaying a marked increase but only reaching $Frac_{POC}$ values of 60% at $Q:Q_m > 10$ (Figure 4c). As was the case for $Frac_{TSS}$, both Elder Creek and Cahto Creek, showed much more moderate increases in $Frac_{POC}$, with values that did not exceed 30% at elevated $Q:Q_m$ conditions. $Frac_{POC}$ also displayed considerable increases with increasing discharge conditions for the Umpqua basin streams (Figure 4d), with the Umpqua River at Elkton showing variable $Frac_{POC}$ contents (50%–70%) at high discharges and Little Wolf Creek showing increases in $Frac_{POC}$ that reached values >70% at the highest $Q:Q_m$ conditions measured. Combined these data illustrate the importance of particulate phases at high discharge levels by all these stream systems (Table 3; Figure S4 in Supporting Information S1).

GOÑI ET AL. 12 of 30

onlinelibrary.wiley.com/doi/10.1029/2022/G007084 by Oregon State University, Wiley Online Library on [05/04/2023]. See the Terms and Conditions (https://onlinelibrary.wiley.

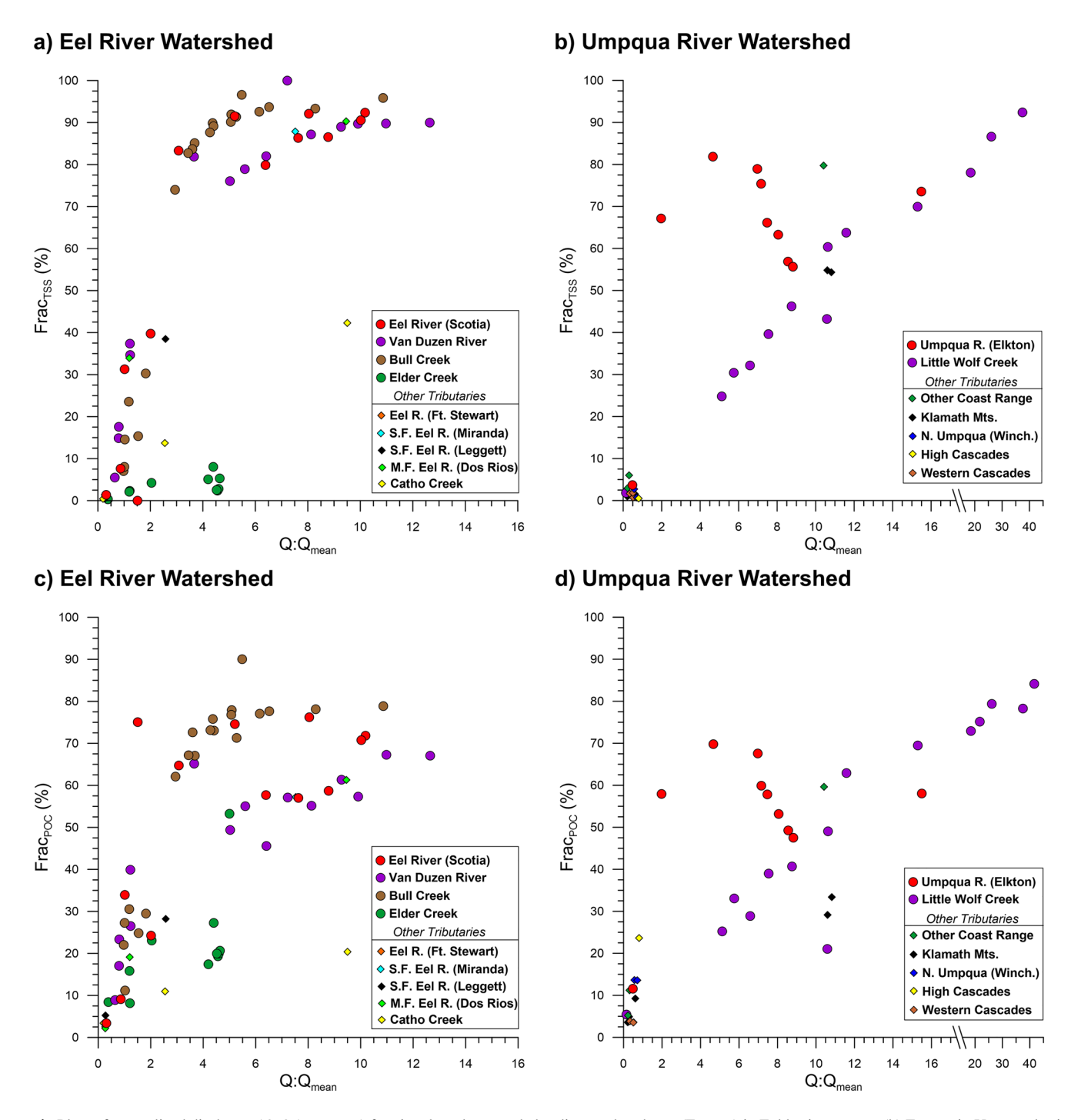


Figure 4. Plots of normalized discharge $(Q:Q_m)$ versus a) fractional total suspended sediment abundance (Frac_{TSS}) in Eel basin streams, (b) Frac_{TSS} in Umpqua basin streams, (c) fractional particulate organic carbon abundance (Frac_{POC}) in Eel basin streams, and (d) Frac_{POC} in Umpqua basin streams.

4.2.2. Particulate and Dissolved Organic Matter Contents

In this study, we use TSS and POC concentrations to calculate the organic matter content of the particulate materials (%POC) exported by these streams under different discharge regimes in both watersheds (see Figures 5a and 5b and Table 3). The data show that in most of these streams increases in discharge led to decreases in the %POC of mobilized particles, despite the fact that both TSS and POC concentrations displayed increases with increased discharge. There were major contrasts between the Eel and Umpqua watershed streams (Figures 5a and 5b), with most of the Eel sites displaying markedly lower %POC values at both low and high $Q:Q_m$ ranges

GOÑI ET AL. 13 of 30

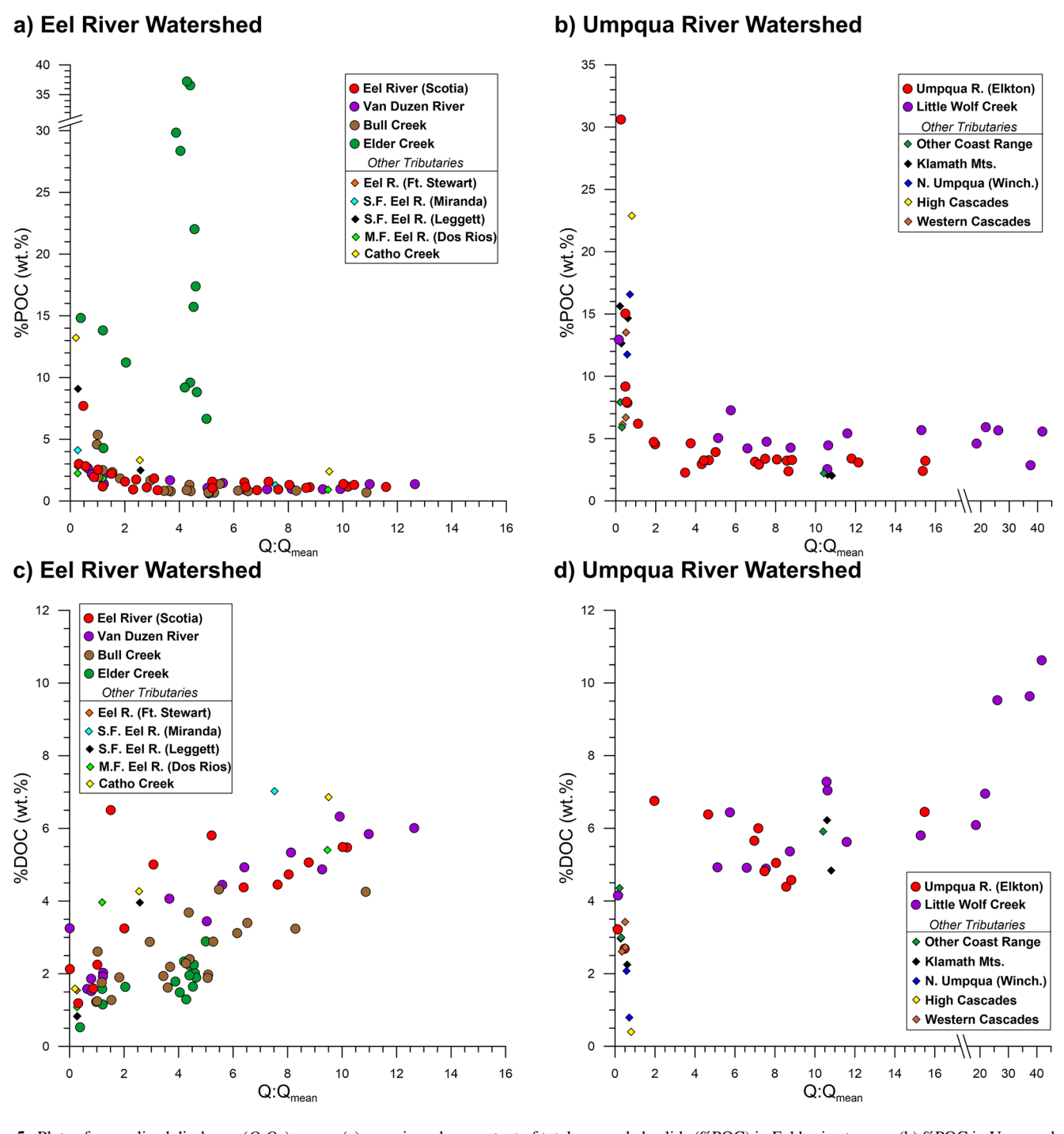


Figure 5. Plots of normalized discharge $(Q:Q_m)$ versus (a) organic carbon content of total suspended solids (%POC) in Eel basin streams, (b) %POC in Umpqua basin streams, (c) organic carbon content of total dissolved solids (%DOC) in Eel basin streams, and (d) %DOC in Umpqua basin streams.

relative to those from the Umpqua River streams (Figure S4c in Supporting Information S1). Thus, whereas samples collected from the Eel River at Scotia, Van Duzen, and Bull Creek at $Q:Q_m < 1$ had %POC < 10%, many of the Umpqua streams displayed %POC between 5% and 25% under similar discharge conditions. At higher ranges of $Q:Q_m$, the Eel River sites displayed uniformly low %POC values (1%–3%) whereas samples from the Umpqua River sites had higher %POC values (2%–8%). Table 3 and Figure S4c in Supporting Information S1 summarize and illustrate these trends among the streams with samples across multiple discharge conditions. The major exception was Elder Creek, in the Eel River basin, which showed uniformly high %POC values (6 to >30%) relative to other stream gage stations in this watershed.

GOÑI ET AL. 14 of 30

 Table 4

 Correlation Coefficients (r) Between Stream Constituent Parameters and Watershed Characteristics

Parameter	Log area	<i>p</i> -value	Slope	p-value	Precipitation	<i>p</i> -value	Runoff	p-value	Erosion	<i>p</i> -value	Log sed yield	<i>p</i> -value
$b_{ m TSS}$	-0.18	0.73	-0.45	0.37	-0.38	0.46	0.28	0.59	0.22	0.68	0.67	0.15
$b_{ m TDS}$	0.01	0.99	0.36	0.49	0.38	0.46	-0.67	0.14	-0.89	0.02	-0.68	0.14
b_{POC}	-0.32	0.99	-0.23	0.54	-0.43	0.39	0.16	0.77	0.21	0.70	0.61	0.20
$b_{ m DOC}$	-0.70	0.12	-0.39	0.45	0.44	0.38	0.67	0.14	0.34	0.51	0.28	0.59
Frac _{TSS}	0.57	0.24	-0.95	0.004	-0.63	0.18	-0.16	0.76	0.62	0.19	0.90	0.01
Frac _{POC}	0.46	0.36	-0.89	0.02	-0.71	0.11	-0.18	0.73	0.43	0.40	0.85	0.03
%POC	-0.55	0.26	0.93	0.01	0.76	0.08	0.28	0.59	-0.54	0.26	-0.84	0.04
%DOC	0.36	0.48	-0.34	0.51	-0.81	0.05	-0.70	0.13	0.15	0.78	0.23	0.66

Note. Watershed characteristics are as defined in Table 1. Parameters are as defined in Tables 2 and 3. Bold numbers identify statistically significant relationships.

As with TSS and POC, the concentrations of TDS and DOC can be used to calculate the percent of the total dissolved load represented by organic carbon (%DOC). In contrast to the pattern observed with %POC, %DOC contents increased with discharge conditions among all streams, from relatively low values of 0.5%-4% at $Q:Q_m < 1$ to values of 2%-7% at $Q:Q_m > 3$ depending on the site (Figures 5c and 5d). Overall, while the contrasts between high- and low-flow %DOC values among streams from the Eel and Umpqua river basins were less pronounced than those displayed by %POC, DOC became a larger component of the total dissolved load in all the rivers sampled in this study as discharge levels increased (Table 3; Figure S4d in Supporting Information S1).

5. Discussion

5.1. Controls on Constituent Concentrations and Compositions

The C-Q relationships for TSS, TDS, POC, and DOC presented above (Figures 2 and 3) can be used to assess their chemostatic and chemodynamic trends that delineate transport-limited versus source-limited behavior (e.g., Moatar et al., 2017). Previous studies investigated the chemodynamic and chemostatic behavior of different stream materials relative to factors such as catchment size and slope, bedrock geology, stream order, mean runoff, mean precipitation, catchment temperature, watershed productivity, and land-cover (e.g., Clark et al., 2022; Creed et al., 2015; Godsey et al., 2009, 2019; Moatar et al., 2017; Mulsoff et al., 2015; Torres et al., 2015). Most of these studies relied on a large data sets collected over a wide range of time scales. In this study, we have a limited number of observations collected during high discharge events that limit our ability to make broad comparisons. However, the six catchments with the largest number of measurements (Eel River, Van Duzen River, Bull Creek, Elder Creek, Umpqua River, and Little Wolf Creek) display significant contrasts in watershed characteristics and a wide range of C-Q slopes (b_{TSS}, b_{TDS}, b_{POC}, b_{DOC}) that are worth exploring. Here, we examine how these variables are statistically related to hypsographic features such as catchment area and slope, hydrologic characteristics such as mean annual precipitation and runoff, and geomorphic attributes such as erosion rate and sediment yield. Table 4 summarizes our findings and supporting figures (Figures S5–S10 in Supporting Information S1) illustrate the patterns.

Our measurements show that TSS-, POC- and DOC-Q relationships across the Eel and Umpqua watersheds yield b values > 1 for the resulting power fits (Table 2), providing a clear indication that these three constituents behave in a way that is consistent with transport limitation. Our findings agree with previous studies that show TSS (e.g., Milliman & Syvitski, 1992; Syvitski et al., 2003), POC (e.g., Beusen et al., 2005; Ludwig & Probst, 1996) and DOC fluxes (e.g., Raymond & Saiers, 2010; Zarnetske et al., 2018) increase with discharge and are influenced by catchment area and basin composition. However, despite the importance that factors such as watershed area, erosion rate, and sediment yield play in determining the overall magnitude of TSS, POC, and DOC fluxes, we do not find statistically significant (p < 0.05) correlations between b_{TSS} , b_{POC} and b_{DOC} values determined from our C-Q relationships and watershed characteristics (Table 4). In the case of TDS, all the stream sites displayed negative b_{TDS} values that were close to zero (Table 2) indicative of near chemostatic behavior, and consistent with slight source limitation and dilution of TDS at high flows. Unlike the other b values, the b_{TDS} exponents display a significant negative relationship with the estimated erosion rates for the six watersheds (Figure S9b in Supporting Information S1). These trends suggest enhanced dilution (more negative b_{TDS}) of chemical weathering products

GOÑI ET AL. 15 of 30

in those catchments where physical erosion rates are greatest (e.g., Van Duzen) relative to those with lower rates (e.g., Umpqua). These findings are consistent with observations in other rivers across the region and around the world (e.g., Bywater-Reyes et al., 2017; Godsey et al., 2009; Meybeck et al., 2003).

The lack of clear statistically significant relationships among C-Q exponents and watershed characteristics likely reflects the reduced sample size in our study, which limits our ability to calculate statistically robust correlation coefficients. Previous studies used much larger regional and national data sets to investigate correlations between b exponents and catchment characteristics such percent of arable land, average annual runoff, mean annual precipitation, and mean catchment slope (e.g., Godsey et al., 2009; Moatar et al., 2017; Torres et al., 2015). In these and other studies with large data sets, statistical significant correlations (p < 0.05) are often found, but their predictive power is low, meaning individual correlations often explain less than 20% of the variance. More recent studies have used nonlinear regression modeling to rank landscape and climatic predictors to the flux parameters. For example, Zarnetske et al. (2018) found wetland extent and evergreen forest extent to be highly predictive variables and positively correlated with the b exponent for DOC across over 1,000 watersheds in the United States. Godsey et al. (2019) used a multiple regression approach to relate catchment characteristics of about 1,200 sites within the United States and Canada and b exponents for a variety of solutes calculated from long-term, mean flow-weighted concentrations. These analyses showed that a variety of lithologic and land cover controls exert influences on the C-Q relationships of most constituents in patterns that were not captured with the event-scale sampling we used in our study.

5.2. Controls on Constituent Compositions

Our measurements show that the contributions of particulate constituents to the total loads of solids (Frac_{TSS}) and of carbon (Frac_{POC}), as well as the carbon contents in both the particulate (%POC) and dissolved (%DOC) phases vary significantly as a function of discharge (Figures 4 and 5). For example, both Frac_{TSS} and Frac_{POC} display considerable increases as a function of discharge with values at low flows ($Q:Q_m < 1$) that are less than 10% and values at high flows ($Q:Q_m > 3$) that exceed 50% in most of the streams (Table 3). In contrast, with increasing discharge most streams exhibit marked decreases in %POC, with values at low flows that range from 2 to 15 wt% and values at $Q:Q_m > 3$ that range from 1 to 5 wt%. The same range of flow regime shows moderate increases in %DOC, with values that range from 0.5 to 4 wt% at $Q:Q_m < 1$ to %DOC values of 2–7 wt.% at $Q:Q_m > 3$ (Table 3). These contrasts in particulate an solute compositions are consistent with previous studies that indicate the sources and characteristics of materials transported during high discharges can be fundamentally different from those mobilized under low discharges, especially by small mountainous river systems (e.g., Clark et al., 2022; Coynel et al., 2005; Creed et al., 2015; Hatten et al., 2012; Lloret et al., 2013; Shanley et al., 2011).

In order to provide context for the observations among the streams in this study, we can examine the same compositional parameters determined in previous studies of much larger rivers such as the Orinoco and Congo (Coynel et al., 2006; Laraque et al., 2013; Moukandi N'kaya et al., 2020). The Orinoco and Congo rivers are large systems characterized by relatively constant hydrographs, similar mean annual discharges, comparable watershed area and similar climate. They differ primarily in the steepness of their watersheds and in their sediment yields, both of which are significantly higher in the Orinoco. The compositional parameters calculated from the TSS, TDS, POC, and DOC concentrations measured in these two systems highlight the contrasts of their suspended and dissolved loads. For example, the material exported by the Orinoco River is characterized by Frac_{TSS} values that range from 45% to 70%, Frac_{POC} values that range from 25% to 50%, %POC values that range from 1 to 8 wt% and %DOC values that range from 8 to 14 wt%. In contrast, Frac_{TSS} values for the Congo River range from 27% to 39% and %DOC values that range from 19 to 27 wt%. The authors of these studies conclude that the higher Frac_{TSS} and lower %DOC values in the Orinoco relative to the Congo reflect the distinct physical and weathering regimes of these two systems. Their results also highlight the relatively muted variability in compositional parameters of these large, continental-scale rivers characterized by relatively constant hydrographs, especially when compared to the trends from the small mountainous river streams in the Eel and Umpqua watersheds (Table 3).

Examination of how the compositions of materials transported at high flows by the Eel and Umpqua streams vary as function of watershed characteristics reveals several statistically significant relationships that are worth highlighting (Table 4). For example, both $\operatorname{Frac}_{TSS}$ and $\operatorname{Frac}_{POC}$ calculated for $Q:Q_m>3$ conditions display significant, negative correlations with basin slope (Figures S6e and S6f in Supporting Information S1) and significant positive relationships with log sediment yield (Figures S10e and S10f in Supporting Information S1). These

GOÑI ET AL. 16 of 30

findings are consistent with observations in other regions that indicate contributions from particulate material sources increase with denudation and physical weathering process (e.g., Bright et al., 2020; Clark et al., 2022). Notably, the overall content of organic content in solid materials (%POC) exported by these watersheds at high flows ($Q:Q_m > 3$) also displays a strong positive correlation with basin slope and a strong negative correlation with log sediment yield (Table 4; Figures S6g and S10g in Supporting Information S1, respectively). These trends are similar to those observed in southern New Zealand, where slope was positively correlated with the organic matter content of particulate materials exported by mountainous river systems in the region (Bright et al., 2020). Furthermore, our observations are consistent with multiple previous studies that showed enhanced contributions from organic-poor soils and bedrock in catchments with higher sediment export (e.g., Galy et al., 2015; Gomez et al., 2010; Hilton & West, 2020; Leithold et al., 2006). The differences in the nature of particulate materials exported from different watersheds at high discharges influences the compositions of land-derived sedimentary materials that accumulate in offshore depocenters (e.g., Hastings et al., 2012; Leithold & Hope, 1999).

Annual precipitation has been shown to be an important factor in controlling the fluxes and compositions of different dissolved and particulate constituents (e.g., Gaillardet et al., 2011; Ludwig & Probst, 1996). Among the compositional parameters calculated for high discharge conditions ($Q:Q_m > 3$; Table 3), %DOC displays statistically significant decreases with increased precipitation (Table 4; Figure S7h in Supporting Information S1). Notably, as discussed above, these trends are not due to dilution of DOC at high flows given the fact our data clearly show concentrations increase with discharge in all the watersheds (Table 3). Instead, these relative depletions in organic matter content at high flows reflect changes in the composition of materials mobilized during high precipitation and suggest the wettest watersheds in our study area export dissolved materials that are relatively depleted in organic matter in comparison to their dryer counterparts. Previous studies have shown DOC to be transport-limited in a majority of U.S. watersheds, spanning multiple ecoregions and climate regions (Zarnetske et al., 2018). These authors identified variables such hydrologic connectivity and water routing as important factors influencing DOC mobilization from different watersheds. Our results are consistent with this finding and suggest wetter watersheds are likely to exhibit different connectivity that influence the composition (e.g., carbon content) of both dissolved and particulate materials mobilized at high flows.

5.3. Flux Calculations

Despite the watershed and climatic controls on constituent concentrations and compositions (see discussion above), discharge itself is often considered a master variable in determining the fluxes of particulate and dissolved constituents by streams (e.g., Raymond & Saiers, 2010; Syvitski et al., 2003). Here, we use the C-Q relationships summarized in Table 2 and apply them to the discharge records from the USGS gage stations to estimate daily fluxes of TSS, TDS, POC, and DOC according to Equation 2. From the daily fluxes, we calculate cumulative fluxes to explore the role of discharge in determining the magnitude and timing material export by these rivers. Figure 6 provides an example of how inter-annual differences in discharge, as well as the magnitude and frequency of individual flood events, affect water, TSS, TDS, POC, and DOC fluxes in Little Wolf Creek. Cumulative fluxes for water, TSS, TDS, POC, and DOC are calculated for each water year (WY = 1 October to 30 September) and plotted for the duration of the study (WY 2015–2016 to 2018–2019). To further illustrate the role of hydrology on the timing of material fluxes, we include two circles in each of cumulative flux panels. The first indicates the time in each WY when 50% of the cumulative flux has been achieved, and the second circle indicates when 90% of the cumulative flux for that specific WY has been reached. Table S2 in Supporting Information S1 provides a summary of these calculations for all six USGS gage stations where we have enough data to determine C-Q trends.

The plots of cumulative fluxes reveal several features that highlight the importance of discharge. For example, among the four water years of the Little Wolf Creek record (Figure 6), WY2016–2017 was the wettest, with multiple flood events that reached mean daily discharges above $\sim 10~\rm m^3~s^{-1}$ and resulted in the highest cumulative annual water flux of $3.6 \times 10^7~\rm m^3$. In contrast, WY2015–2016 and WY2018–2019 were characterized by fewer events that led to lower cumulative water fluxes of $2.3 \times 10^7~\rm m^3$, respectively. Finally, WY2017–2018 was the driest of the 4 yr with small flood events that did not reach daily fluxes above 5 m³ s⁻¹ and a cumulative water flux of $1.3 \times 10^7~\rm m^3$. Among the calculated material fluxes, those of TDS and DOC display trends comparable to the cumulative water fluxes, reflecting the fact that these constituents were characterized by lower *b* exponents in the *C-Q* relationship. Thus, as is the case for cumulative water flux, WY2016–2017 has

GOÑI ET AL. 17 of 30

21698961, 2023, 4, Downloaded from https://agupubs.onlinelibrary.wiley.com/doi/10.1029/2022JG007084 by Oregon State University, Wiley Online Library on [05/04/2023]. See the Terms and Conditions (https://onlinelibr

Little Wolf Creek USGS 14320934

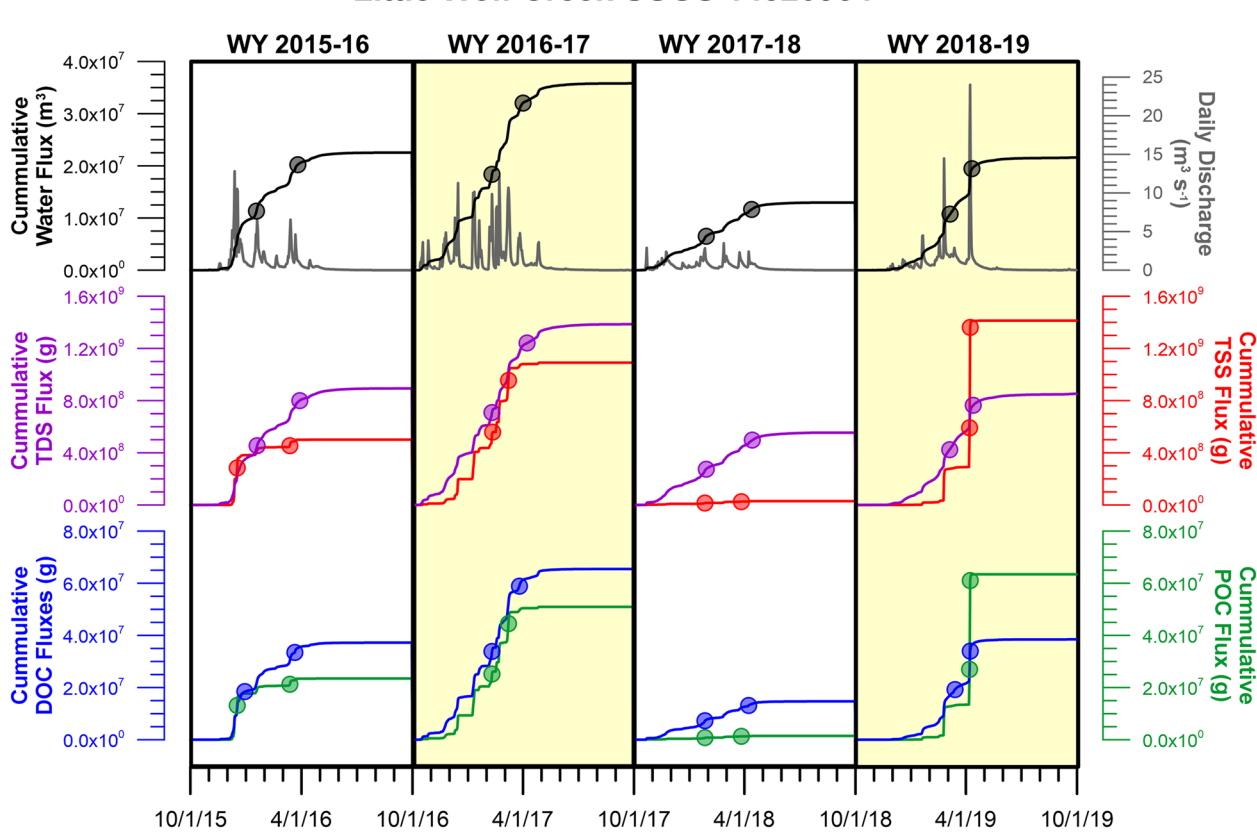


Figure 6. Daily and cumulative water discharges, and cumulative discharges of total suspended solids (TSS), total dissolved solids (TDS), particulate organic carbon (POC), and dissolved organic carbon (DOC) for Little Wolf Creek during water years 2015–2016, 2016–2017, 2017–2018, and 2018–2019. The text provides details of how the flux calculations were made based on USGS stream gage data and *C-Q* relationships determined in this study. The circles in each cumulative flux plot indicate the days when 50% and 90% of the cumulative flux was achieved for each material.

the highest TDS and DOC cumulative fluxes $(1.4 \times 10^9 \text{ g} \text{ and } 6.6 \times 10^7 \text{ g}, \text{respectively})$, whereas WY2017–2018 has the lowest TDS and DOC cumulative fluxes $(5.5 \times 10^8 \text{ g} \text{ and } 1.5 \times 10^7 \text{ g}, \text{respectively})$. WY2015–2016 and WY2018–2019 show intermediate TDS and DOC cumulative fluxes with comparable trends to those of water, which reflect the more chemostatic nature of the transport of these materials in the Little Wolf Creek system (as well as in other streams in both the Eel and Umpqua river system; Table S2 in Supporting Information S1).

The trends in the fluxes of dissolved constituents are in stark contrast to particulate constituents (TSS and POC), which are characterized by high b exponents and transport limited behavior in their mobilization from the catchment area. Hence, unlike TDS and DOC, the highest cumulative fluxes of TSS and POC $(1.4 \times 10^9 \text{ g})$ and 6.3×10^7 g, respectively) occur during WY2018–2019 and are significantly higher than the cumulative fluxes during WY2016–2017 (1.1×10^9 g and 5.1×10^7 g, respectively) despite the latter having a considerably higher cumulative water flux (Figure 6). The differences in particulate fluxes between WY2018–2019 and WY2016– 2017 are a direct result of the high-magnitude flood event (mean daily flux >20 m³ s⁻¹) that took place in mid-April of 2019 and which dominates the flux of particulate constituents with high transport limited behavior. Because dissolved constituents such as TDS and DOC display more chemostatic behavior; this flood event has a small impact on their overall flux. Another example of the importance of flood magnitude in export of particulate constituents by these streams is the much lower cumulative TSS and POC fluxes calculated for WY2015-2016 $(5.0 \times 10^8 \text{ g} \text{ and } 2.3 \times 10^7 \text{ g}, \text{ respectively})$, which has comparable water discharge than WY2018–2019 but was characterized by only a couple of flood events with mean daily discharges of ~10 m³ s⁻¹. Other stream systems in both the Eel and Umpqua watersheds display comparable trends in cumulative discharges (Table S2 in Supporting Information S1), reinforcing the importance of flood events have in determining the magnitude and timing of material fluxes (TSS, POC, and DOC to a lesser degree) from these small mountainous watersheds. Our results

GOÑI ET AL. 18 of 30

21698961, 2023, 4, Download

are consistent with many other studies that highlight the role of high discharge events in fluvial material export (e.g., Clark et al., 2022; Dhillon & Inamdar, 2014; Goñi et al., 2013).

Discharge not only plays a critical role in the magnitude of material fluxes, it also has a fundamental impact on their timing, both of which influence the ultimate fate of materials exported from watersheds (e.g., Geyer et al., 2004; Walsh & Nittrouer, 2009). Thus, for example, in all the streams of this study, TDS and water display similar periods required to achieve 50% and 90% of their respective annual fluxes (Table S2 in Supporting Information S1). As illustrated by the example of Little Wolf Creek, it takes between 178 and 196 days to reach 90% of the total cumulative water or TDS fluxes depending on the specific water year (Figure 6). Constituents with transport-limited behavior display considerable shorter periods to achieve 50% and 90% of total annual fluxes because of the steeper *C-Q* relationships and the predominant role of flood events. Hence, the periods to reach 90% of total annual flux of DOC in Little Wolf Creek are shorter (173–190 days) than for TDS and water, but longer than those required to reach 90% of annual TSS and POC fluxes (159–190 days; Figure 6). All other streams in the Eel and Umpqua basins have similar trends in the period of time required to achieve 50% and 90% of material fluxes (Table S2 in Supporting Information S1). These contrasts in the timing of cumulative fluxes imply that not all materials exported from small mountainous watersheds are delivered simultaneously. Because of the significant temporal differences in offshore conditions, these temporal offsets have the potential to influence the physical transport and biogeochemical fate of fluvial materials in the coastal ocean.

Furthermore, there are marked inter-annual differences in the timing of delivery of materials by each of these streams (e.g., Table S2 in Supporting Information S1). For example, in the case of Little Wolf Creek (Figure 6), WY2015-2016, WY2016–2017, and WY2017–2018, which were characterized multiple flood events during the wet season (November–April), show more uniformly distributed fluxes with multiple weeks (26–75 days depending on constituent and year) separating the dates when 50% and 90% fluxes are achieved. This more distributed flow regime is in stark contrast to WY2018–2019 when one large flood event dominates the flow regime. In the case of Little Wolf Creek, WY2018–2019 is characterized by temporal difference between 50% and 90% fluxes that are much shorter, especially for transport-limited constituents such as TSS and POC. For these constituents, the period between 50% and 90% flux is reduced to 1 day (Figure 6). Hence, the timing in the export of transport-limited constituent fluxes (e.g., TSS and POC) is highly dependent on flood events, meaning long-term discharge averages are poor predictors of not only the overall quantity of export fluxes but also the timing and seasonality of their delivery.

5.4. River Fluxes and Compositions Relative to Coastal Ocean Conditions

In order to evaluate the potential fates of land-derived materials once they enter the ocean, we can examine the timing and magnitude of river fluxes at the most downstream gage stations and contrast them to offshore conditions. Figures 7 and 8 illustrate this approach by plotting the time-series of daily discharge and the cumulative fluxes of water, TSS, TDS, POC, and DOC in the same scale as north-south wind speeds and wave heights measured offshore of the Eel and Umpqua river mouths. In the same fashion as Figure 6, the dots in each graph indicate the date when 50% and 90% of the annual cumulative flux of each constituent is reached for each water year. We note that while rivers are important sources of many constituents, their impacts on marine biogeochemical cycles of the coastal ocean regions can be varied. For example, terrestrial POC and DOC inputs can represent important sources of organic matter to ocean ecosystems, especially during periods when autochthonous productivity is limited (e.g., Kieft et al., 2020; Thomsen et al., 2017; Wetz et al., 2006). On the other hand, the impacts of TSS and TDS are more difficult to ascertain because they represent the sum of different materials (e.g., clay vs. silt particles) and chemicals (e.g., silicate, bicarbonate) with distinct relevant roles in coastal ecosystems. In this study, we focus on the magnitude and timing of bulk TSS and TDS fluxes; however, Ghazi et al. (2022) provide flux information on individual solutes that contribute to the TDS patterns discussed here.

It is important to note that estuarine processes (e.g., mixing, deposition, transformation) can alter the magnitude, timing, and composition of materials entering the ocean (e.g., Ward et al., 2017). Thus, the trends illustrated in these graphs should be considered in the context of estuarine influences on fluvial fluxes. However, as most other mountainous coastal rivers worldwide, the Eel and Umpqua rivers have relatively small estuaries (~0.2% of total basin area) compared to other major river systems. Thus, estuarine processes in small mountainous rivers, such as the ones along the west coast of the U.S., play a smaller role in modulating material export to the ocean (e.g., Goni et al., 2014; Gray et al., 2016; Peck et al., 2020), especially under high discharge conditions when fluvial-derived materials are effectively transported offshore (e.g., Geyer et al., 2004; Pullen & Allen, 2001; Walsh & Nittrouer, 2009).

GOÑI ET AL. 19 of 30

21698961, 2023, 4, Downloaded from https://agupubs.onlinelibrary.wiley.com/doi/10.1029/2022/G007/084 by Oregon State University, Wiley Online Library on [05/04/2023]. See the Terms and Conditions (https://onlinelibrary.wiley.com/terms-and-conditions) on Wiley Online Library for rules of use; OA articles are governmentally on [05/04/2023]. See the Terms and Conditions (https://onlinelibrary.wiley.com/terms-and-conditions) on Wiley Online Library for rules of use; OA articles are governmentally on [05/04/2023]. See the Terms and Conditions (https://onlinelibrary.wiley.com/terms-and-conditions) on Wiley Online Library for rules of use; OA articles are governmentally on [05/04/2023]. See the Terms and Conditions (https://onlinelibrary.wiley.com/terms-and-conditions) on Wiley Online Library for rules of use; OA articles are governmentally on [05/04/2023]. See the Terms and Conditions (https://onlinelibrary.wiley.com/terms-and-conditions) on Wiley Online Library for rules of use; OA articles are governmentally on [05/04/2023]. See the Terms and Conditions (https://onlinelibrary.wiley.com/terms-and-conditions) on Wiley Online Library for rules of use; OA articles are governmentally on [05/04/2023]. See the Terms and Conditions (https://onlinelibrary.wiley.com/terms-and-conditions) on Wiley Online Library for rules of use; OA articles are governmentally on [05/04/2023]. See the Terms and Conditions (https://onlinelibrary.wiley.com/terms-and-conditions) on [05/04/2023]. See the Terms and Conditions (https://onlinelibrary.wil

Eel River @ Scotia USGS 11477000

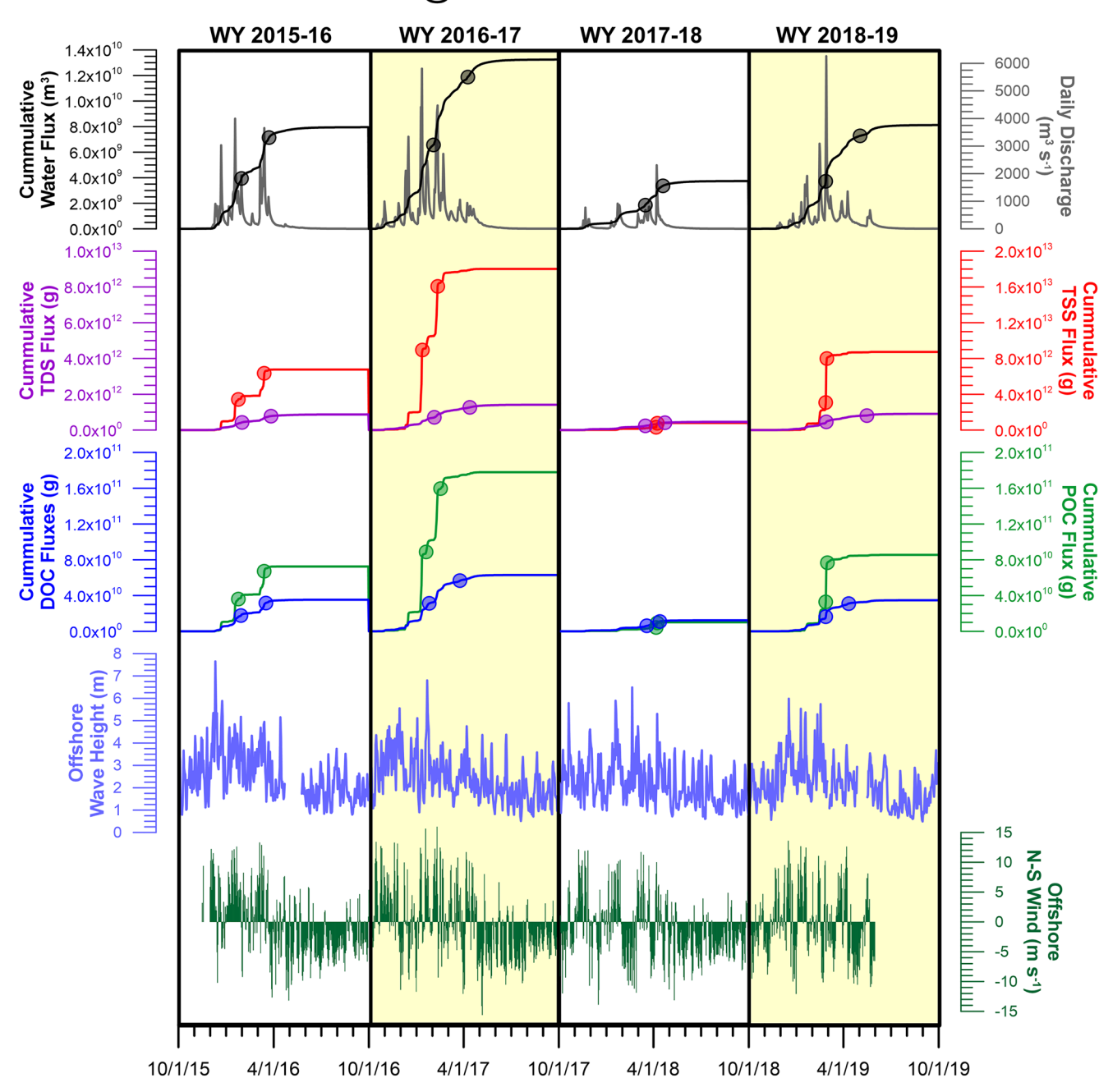


Figure 7. Daily and cumulative water discharges, and cumulative discharges of total suspended solids (TSS), total dissolved solids (TDS), particulate organic carbon (POC), and dissolved organic carbon (DOC) for Eel River at Scotia during water years 2015–2016, 2016–2017, 2017–2018, and 2018–2019. Also included in the graphs are time-series plots of wave height and north-south wind speeds based on observations from a NOAA buoy offshore the Eel River mouth. The text provides details of how the flux calculations were made based on USGS stream gage data and *C-Q* relationships determined in this study. The circles in each cumulative flux plot indicate the days when 50% and 90% of the cumulative flux was achieved for each material.

5.4.1. Seasonal and Inter-Annual Contrasts

Both the Eel and Umpqua rivers are characterized by stark seasonal contrasts in water discharge and material fluxes associated with wintertime atmospheric patterns that control precipitation. Figures 7 and 8 illustrate the inter-annual variability within each system and highlight the differences in flux behavior between the Eel and the Umpqua rivers. The wet season totals computed in Table S3 in Supporting Information S1 show the importance of this period, which we define here from 1 December to 15 April, in the delivery of land-derived materials

GOÑI ET AL. 20 of 30

Umpqua River @ Elkton USGS 14321000

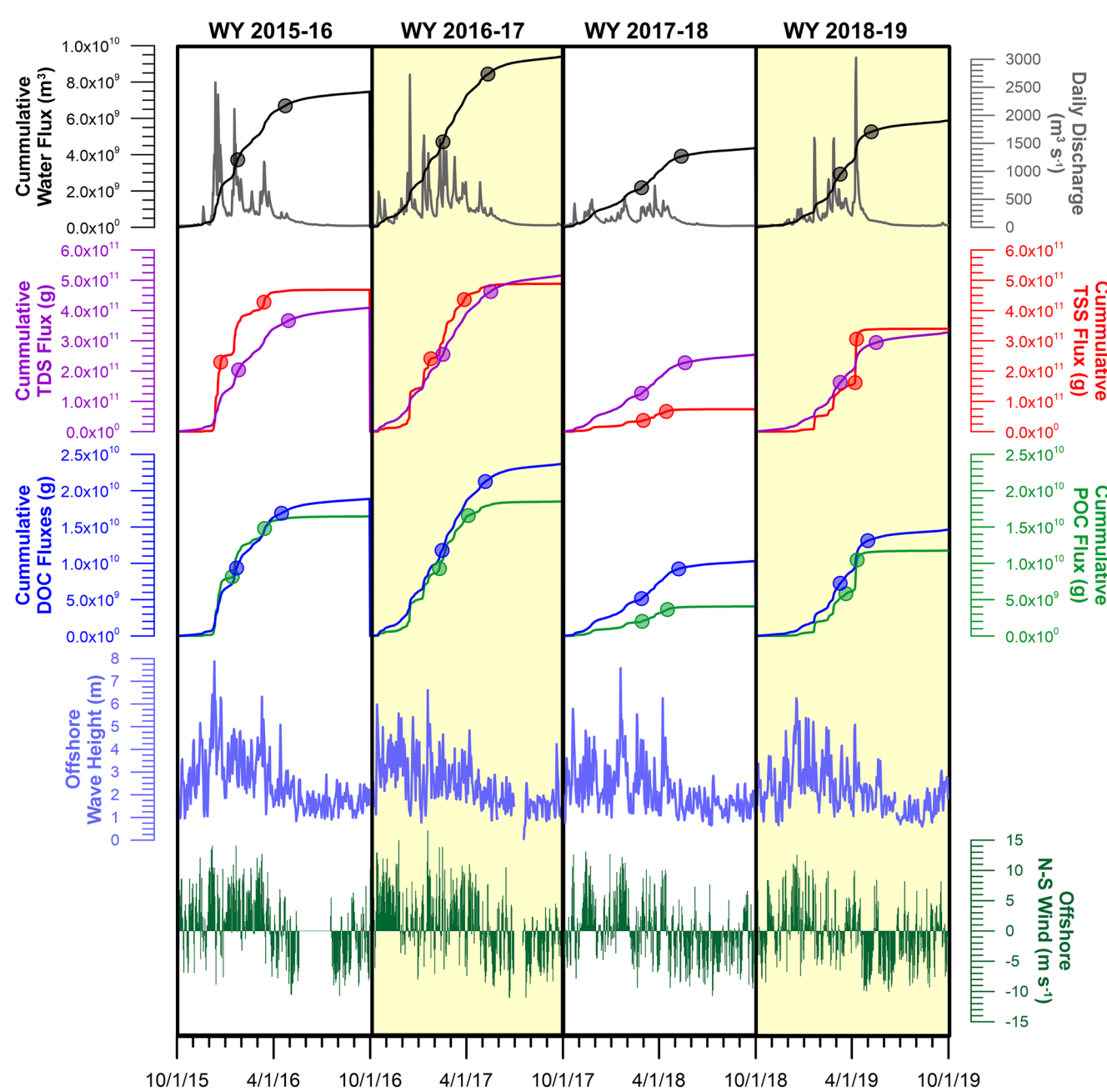


Figure 8. Daily and cumulative water discharges, and cumulative discharges of total suspended solids (TSS), total dissolved solids (TDS), particulate organic carbon (POC), and dissolved organic carbon (DOC) for Umpqua River at Elkton during water years 2015–2016, 2016–2017, 2017–2018, and 2018–2019. Also included in the graphs are time-series plots of wave height and north-south wind speeds based on observations from a NOAA buoy offshore the Umpqua River mouth. The text provides details of how the flux calculations were made based on USGS stream gage data and *C-Q* relationships determined in this study. The circles in each cumulative flux plot indicate the days when 50% and 90% of the cumulative flux was achieved for each material.

(water, TSS, TDS, POC, and DOC) to the ocean. Hence, for example, while the wet season only represents 37% of each water year, it accounts from 78% to 95% (depending on the year) of water discharge by the Eel River (Figure 7; Table S3 in Supporting Information S1). In the case of the Umpqua River, the same wet season period accounts for lower percentages of annual total river discharge (60%–84%; Figure 8; Table S3 in Supporting Information S1), illustrating the more distributed behavior of fluvial flows in this system. Because of the steep C-Q relationships exhibited by TSS and POC in the Eel River, the wet season accounts from 94% to 100% of

GOÑI ET AL. 21 of 30

the fluxes of these particulate constituents. In the case of DOC, which in the Eel exhibited lower chemodynamic behavior, the wet season fluxes account for slightly lower percentages of the annual flux (84%–98%), whereas the chemostatic behavior of TDS means wet season fluxes of this component of the fluvial load are basically the same as for water (76%–94% depending on the year; Figure 7; Table S3 in Supporting Information S1). In the case of the Umpqua River, wet season fluxes among the four constituents display similar patterns, with the highest percentages of annual flow for TSS and POC (68%–98%), followed by DOC (61%–86%) and TDS (59%–82%). Overall, wet season fluxes in the Umpqua River are lower than in the Eel River. Again, these results highlight contrasts in the seasonality of different material fluxes between the two systems (e.g., Goñi et al., 2013) beyond the inter-annual variations expected from variable discharge conditions.

In terms of the overall magnitudes of cumulative fluxes, Figures 7 and 8 illustrate the marked contrasts between the Eel and Umpqua rivers regarding the contributions of particulate and dissolved loads. In the case of the Eel River, TSS and POC cumulative fluxes dominate their dissolved counterparts (TDS and DOC) in all but one of the water years (WY2017–2018; Figure 7). This trend is consistent with the characteristics of this river basin, which include large sediment yields related to the elevated tectonic uplift and high erosion rates in most regions of its watershed. Notably, the cumulative flux estimates highlight the importance of high discharge conditions in accentuating this pattern. In contrast, the Umpqua River cumulative discharge trends exhibit much more comparable estimates for particulate and dissolved fluxes for both bulk solids (TSS and TDS) and organic carbon (POC and DOC; Figure 8). The more balanced particulate and dissolved cumulative transport estimates reflect the lower sediment yields, tectonic uplift, and erosion rates in this watershed relative to the Eel system. As illustrated by the patterns in WY2017–2018, discharge plays a significant role in this system as well, leading to significantly lower cumulative fluxes of particulate materials during this relatively dry year.

5.4.2. Patterns With Ocean Conditions

Figures 7 and 8 illustrate the strong seasonal contrasts in water discharge, offshore N-S winds, and wave heights that characterize the Eel and Umpqua river-coastal systems. In both systems, the wet season occurs during winter and early spring (November-April) and is characterized by elevated river discharges, downwelling-favorable southerly winds and elevated wave heights at both locations. The dry summer and early fall months (May-October) are characterized by very low river discharge, upwelling-favorable winds, and decreased wave heights in both the Eel and Umpqua margins. The seasonal patterns are interrupted by shorter-time scale events, which during the wet season in winter include discharge pulses (i.e., floods) that are often accompanied by short-term reversals in winds and periods of elevated waves. Detailed examination of the coherence among these event-based phenomena and fluvial discharges is beyond the scope of this study (e.g., Kniskern et al., 2011), but it is clear that the bulk of material transport by coastal rivers such as the Eel and Umpqua onto the Pacific Northwest margin occurs under conditions that are much different than those that characterize the upwelling-dominated, highly productive spring and summer seasons (e.g., Goñi et al., 2021; Henderikx Freitas et al., 2018; Saldias et al., 2020). Thus, in both the Eel and Umpqua margins, most of the TSS, POC, and DOC fluxes are delivered by the rivers during the winter season, with 90% of the cumulative fluxes typically being achieved by March or April. Variations in the timing of these fluxes are directly related to the frequency and magnitude of seasonal floods. In contrast, 90% cumulative TDS and water fluxes are reached later in the water year, typically in May or June.

The seasonality of river material fluxes means that in the case of the Eel, 70% of the TSS and POC fluxes occur under conditions of moderate to strong downwelling and moderate to high wave-energy (>2 m), which represent on average about 28% of the period covered in this study (WY 2015–2019). In contrast, 60% of the DOC is transported to the coast under these conditions, while 55% of the water and 53% of the TDS are delivered to the coast during this period. Similar estimates for the Umpqua system show that conditions of moderate to strong upwelling-favorable winds and moderate to high wave energy represent 35% of the study period, and account for 53% of TSS and POC being delivered by the Umpqua River. The less skewed behavior in the Umpqua extends to the other constituents (DOC, water, and TDS), which display ~50% of the total fluxes being delivered during these conditions. These contrasts in river-ocean coherence between the Eel and Umpqua rivers extend to other fluvial systems along the west coast of the U.S. (e.g., Kniskern et al., 2011; Pullen & Allen, 2001) and need to be incorporated in regional models of carbon cycling in coastal systems (e.g., Benway et al., 2016; Fennel et al., 2019).

Given the trends observed, we can expect that the majority of the particulate constituents exported by these rivers, especially in the Eel, enter the coastal ocean under conditions that favor northerly along-shore transport

GOÑI ET AL. 22 of 30

and prevent settling in the shallow, nearshore regions of the shelf. The impacts of these forcings can be seen in the winter-time distribution of salinity, TSS and POC along the central Oregon coast (Goñi et al., 2021; Mazzini et al., 2014; Saldias et al., 2020) and the distribution of fluvial depocenters along the Eel and Umpqua mid-shelves (e.g., Wheatcroft & Borgeld, 2000; Wheatcroft et al., 2013). We speculate that the narrower time-window and tighter coherence of particulate discharges by the Eel relative to the Umpqua may contribute to more efficient burial in the former relative to the latter (Hastings et al., 2012; Leithold & Hope, 1999). Contrasts in the composition and reactivity of the suspended load between these two systems likely also contributes to differences in burial efficiencies between the two depocenters. On the other hand, because DOC fluxes and especially TDS fluxes occur over wider periods and ocean conditions, we can expect their transport and delivery to the coastal margins of Northern California and central Oregon to be more variable in both spatial and temporal scales. Such variability is likely to contribute to the more effectively uptake and recycling of these land-derived dissolved constituents relative to their particulate counterparts (e.g., Kieft et al., 2018, 2020).

We note that TDS is a bulk parameter that includes solutes, such as calcium and sodium with fluvial concentrations that are much lower than those in ocean waters and thus likely have negligible impacts in coastal processes. However, TDS also includes of other solutes, such as bicarbonate and silica, which play important roles in the biogeochemistry (e.g., alkalinity, diatom production) of coastal waters and can be impacted by the magnitude and timing of fluvial inputs. Detailed examination of the role of individual TDS components is beyond the scope of this paper. However, the reader is directed to the paper by Ghazi et al. (2022), which lists the *b* exponents of individual chemical species (including nutrients) for both the Eel and Umpqua rivers, and which can be used to assess the behavior of these constituents relative to the trends in TSS, TDS, POC, and DOC fluxes discussed here.

5.4.3. Compositional Trends

Because of differences in the timing of constituent transport by both the Eel and Umpqua rivers (Figures 7 and 8), the compositions of these materials change significantly at seasonal and event-scales. To illustrate these contrasts, we used the daily concentration data used to compute the daily flux data in Figures 7 and 8 to calculate the four compositional parameters previously discussed, Frac_{TSS}, Frac_{POC}, %POC, and %DOC and plot them in the same time scale as the offshore wind and wave data (Figures 9 and 10). To account for the time lag between the compositions calculated at the USGS gage stations in Scotia and Elkton and the conditions measured offshore the Eel and Umpqua river mouths, we plot the composition parameters using 7-day running averages.

The plots in Figures 9 and 10 reveal marked differences in the compositions of materials exported by the two rivers. Thus, for example, in the Eel system, winter floods lead to fluvial material export being dominated by particulate phases, with estimated Frac_{TSS} and Frac_{POC} values during this period that range from 50% to 100% and 40% to 80%, respectively (Figure 9). In contrast, in the Umpqua system, Frac_{TSS} and Frac_{POC} values during high-flow winter conditions both range from 20% to 50%, with only the highest flood events displaying values that reached 60% (Figure 10). Thus, under downwelling-favorable and high wave-energy conditions, land-derived materials exported by Eel are primarily particle-bound, whereas in the Umpqua system dissolved materials contribute significantly to the total material delivered during these periods. Notably, WY2017-2018, which was characterized by reduced flows in both systems resulted in markedly diminished contributions of particulate materials to the overall fluvial export. Furthermore, the carbon contents of the particulate loads during downwelling-favorable periods are consistently lower (%POC values of 1–2 wt.% in the Eel and 3 –7 wt.% in the Umpqua) than those transported during upwelling-favorable, spring-summer conditions (%POC of 3-5 wt.% in Eel and 8 –14 wt.% in the Umpqua; Figures 9 and 10). The carbon contents of the dissolved load show opposite trends, with winter-time, downwelling-favorable periods being characterized by elevated %DOC contents in both the Eel (3%-7%) and Umpqua (4%-5%) rivers relative to compositions during spring-summer, upwelling favorable periods (average %DOC values of 1 and 3 wt.%, respectively).

These trends highlight the marked seasonal and event-based variability in the composition and quality of the land-derived POM and DOM exported by these river systems. They also highlight how the factors that control the composition of materials exported by small mountainous rivers likely play a role in determining the fate of land-derived, fluvial-transported materials delivered by different systems (e.g., Blair & Aller, 2012). The compositional contrasts between most of the Eel and Umpqua streams are linked to the underlying geology and the hydrologic (precipitation/runoff) and geomorphic characteristics (tectonic uplift, erosion, and sediment yield) of their watersheds. As demonstrated by previous studies, streams within the Eel River system mobilize significant amounts of petrogenic carbon, whereas those from the Umpqua system do not (e.g., Goñi et al., 2013; Leithold et al., 2006).

GOÑI ET AL. 23 of 30

21698961, 2023, 4, Downloaded from https://agupubs.onlinelibrary.wiley.com/doi/10.1029/2022/G007084 by Oregon State University, Wiley Online Library on [05/04/2023]. See the Terms and Conditions (https://onlinelibrary.wiley.com/terms-and-conditions) on Wiley Online Library or for use; OA arcites are governed by the applicable Creative and Conditions (https://onlinelibrary.wiley.com/terms-and-conditions) on Wiley Online Library or for use; OA arcites are governed by the applicable Creative and Conditions (https://onlinelibrary.wiley.com/terms-and-conditions) on Wiley Online Library or for use; OA arcites are governed by the applicable Creative and Conditions (https://onlinelibrary.wiley.com/terms-and-conditions) on Wiley Online Library or for use; OA arcites are governed by the applicable Creative and Conditions (https://onlinelibrary.wiley.com/terms-and-conditions) on Wiley Online Library or for use; OA arcites are governed by the applicable Creative and Conditions (https://onlinelibrary.wiley.com/terms-and-conditions) on Wiley Online Library or for use; OA arcites are governed by the applicable Creative and Conditions (https://onlinelibrary.wiley.com/terms-and-conditions) on Wiley Online Library or for use; OA arcites are governed by the applicable Creative and Conditions (https://onlinelibrary.wiley.com/terms-and-conditions) on Wiley Online Library or for use; OA arcites are governed by the applicable of the arcites are governed by the applicable of the arcites are governed by the applicable of the arcites are governed by the arcites are gove

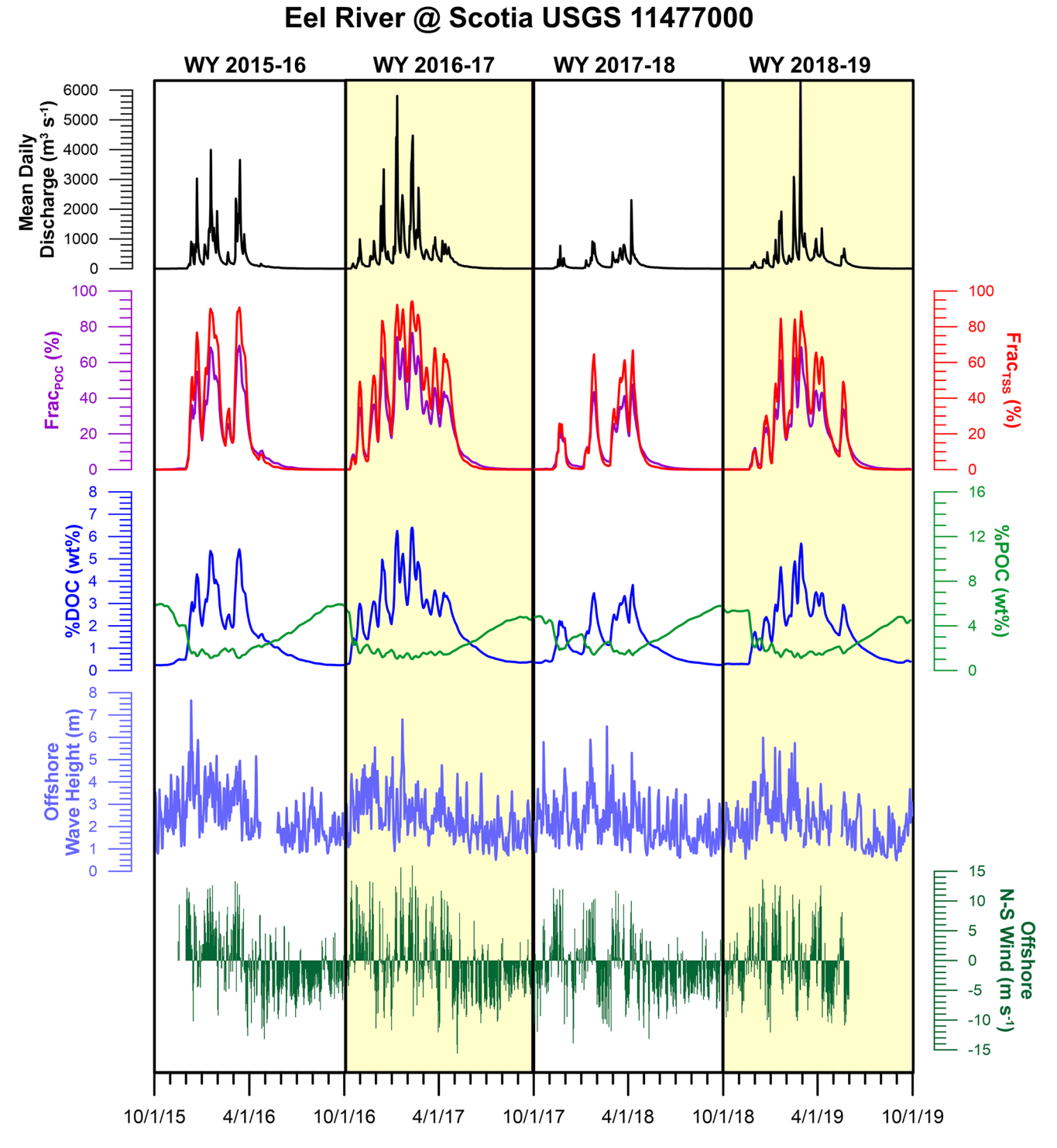


Figure 9. Time-series of daily discharge and 7-day running averages of compositional parameters determined for Eel River at Scotia during water years 2015–2016, 2016–2017, 2017–2018, and 2018–2019. The parameters were calculated from daily concentration data and include fractional total suspended sediment abundance (Frac_{TSS}), fractional particulate organic carbon abundance (Frac_{POC}), organic carbon content of total suspended solids (%POC), and organic carbon content of total dissolved solids (%DOC). Also included in the graphs are time-series plots of wave height and north-south wind speeds based on observations from a NOAA buoy offshore the Eel River mouth. The text provides details of how the compositional parameters were calculated based on USGS stream gage data and *C-Q* relationships determined in this study.

GOÑI ET AL. 24 of 30

21698961, 2023, 4, Downloaded from https://agupubs.onlinelibrary.wiley.com/doi/10.1029/2022/G007084 by Oregon State University, Wiley Online Library on [05/04/2023]. See the Terms and Conditions (https://onlinelibrary.wiley.com/terms-and-conditions) on Wiley Online Library or Trules of use; OA arcicles are governed by the applicable Creative

Umpqua River @ Elkton USGS 14321000

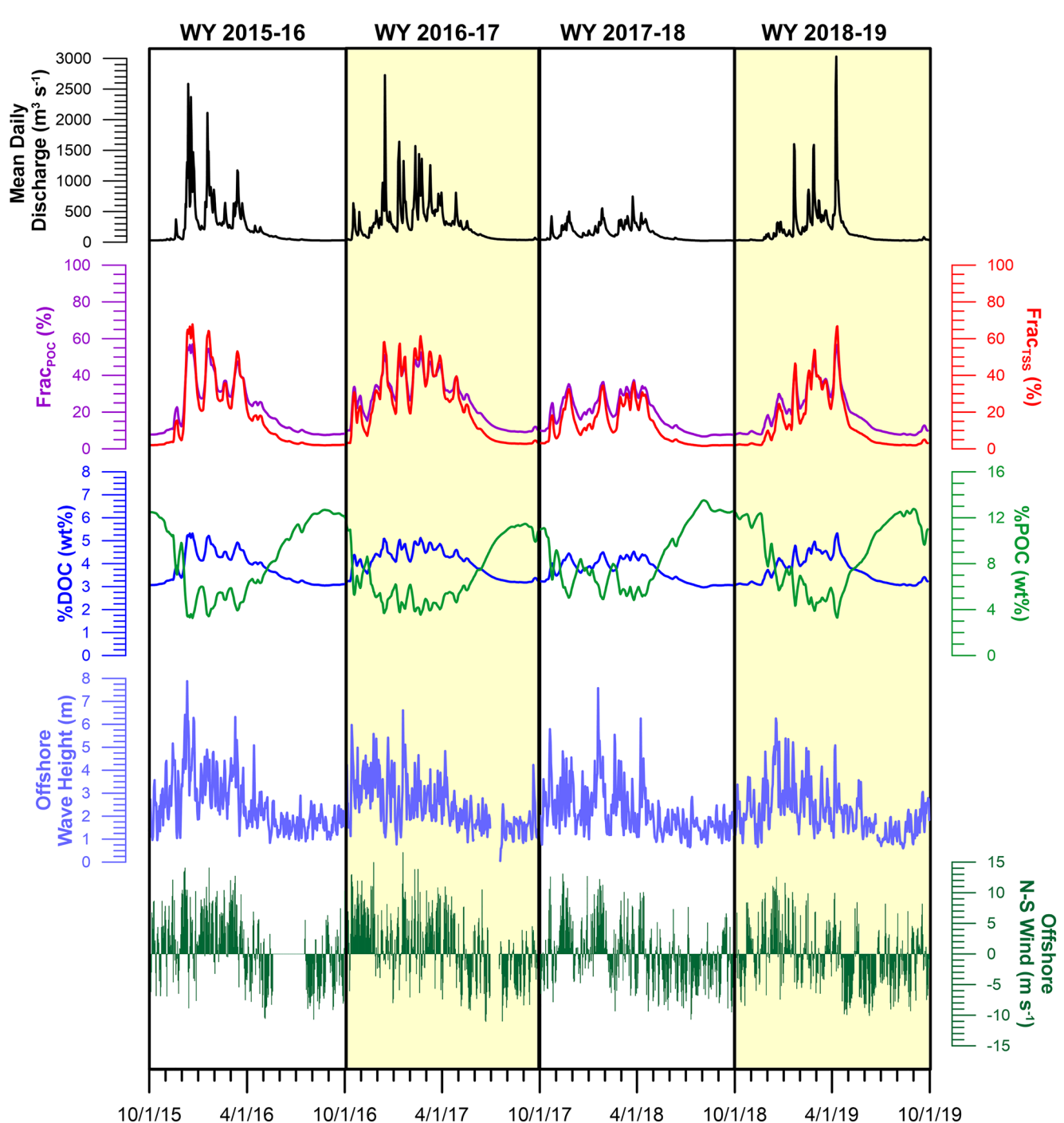


Figure 10. Time-series of daily discharge and 7-day running averages of compositional parameters determined for Umpqua River at Elkton during water years 2015–2016, 2016–2017, 2017–2018, and 2018–2019. The parameters were calculated from daily concentration data and include fractional total suspended sediment abundance (Frac_{TSS}), fractional particulate organic carbon abundance (Frac_{POC}), organic carbon content of total suspended solids (%POC), and organic carbon content of total dissolved solids (%DOC). Also included in the graphs are time-series plots of wave height and north-south wind speeds based on observations from a NOAA buoy offshore the Umpqua River mouth. The text provides details of how the compositional parameters were calculated based on USGS stream gage data and *C-Q* relationships determined in this study.

GOÑI ET AL. 25 of 30

The distinct contributions from less reactive petrogenic carbon relative to more reactive biospheric carbon, combined with the contrasting transport behavior and coherence with ocean conditions between the Eel and Umpqua rivers contribute to determine the fate of land-derived carbon in these and other similar source-to-sink systems. The seasonal and inter-annual contrasts in %DOC may also have important implications for the mobilization and transport of trace metals (such as iron) from coastal watersheds to the ocean. The variability in the concentration, relative abundance, and composition of DOM in waters from both the Eel and Umpqua suggest there may be broad differences in the concentrations and types of organic ligands that are associated with trace metal dissolution and transport (e.g., Kolesnichenko et al., 2021) and should be considered in studies of trace element biogeochemistry along ocean margins (e.g., Zitoun et al., 2021). Far from providing definite answers, our results highlight the importance of the complex interactions between compositional variability and the timing of fluvial fluxes relative to ocean conditions when evaluating the fate of terrigenous materials in ocean margins (e.g., Ausín et al., 2021; Zhao et al., 2021).

6. Summary

Our study characterizes the concentration-discharge relationships of TSS, TDS, POC, and DOC of contrasting streams within two mountainous river systems, the Eel and Umpqua rivers, along the west coast of the USA. The measurements across a range of discharges in each of these systems reveal marked contrasts in the concentration and composition of particulate and dissolved constituents, within and among the studied streams. There are significant differences in the behavior of particulate constituents (TSS and POC) as a function of discharge relative to those of dissolved constituents (TDS and DOC) that highlight the importance of high discharge events (i.e., floods) in the transport and mobilization of the former. Our analyses show statistically significant trends among watershed characteristics (e.g., slope, sediment yield) and specific compositional characteristics of particulate and dissolved constituents, which provide insights into factors controlling material export from mountainous watersheds. Using the C-Q relationships established from the stream samples, we calculate material fluxes (i.e., water, TSS, TDS, POC, and DOC) from several streams within the Eel and Umpqua basins over the four water years (2015-2019) of the study. Our analyses show the highly seasonal nature of material transport in these systems, the inordinate impact of floods on the transport of particulate materials and the critical role of discharge in determining the magnitude and timing of material fluxes. Examination of flux and compositional data from the most downstream gages in the Eel and Umpqua rivers in comparison to physical conditions (winds and waves) offshore illustrate the role that the timing of fluvial delivery plays in the distribution and ultimate fate of fluvial materials along these margins.

Data Availability Statement

All the concentration data for all the samples collected from the different stream gage stations are tabulated in Table S1 in Supporting Information S1 and archived at the hydroshare archival site (see Goni et al., 2022). The complete dissolved solute chemistry data set is also available at the hydroshare archival site (Ghazi et al., 2022). River discharge data are available through the USGS National Water Information System (https://waterdata.usgs.gov/nwis). All wind and wave data are available through NOAA's National Buoy Data Center portal (https://www.ndbc.noaa.gov/).

References

- Aalto, K. R., McLaughlin, R. J., Carver, G. A., Barron, J. A., Sliter, W. V., & McDougall, K. (1995). Uplifted Neogene margin, southernmost Cascadia-Mendocino triple junction region, California. *Tectonics*, 14(5), 1104–1116. https://doi.org/10.1029/95tc01695
- Anderson, T. R., Rowe, E. C., Polimene, L., Tipping, E., Evans, C. D., Barry, C. D. G., et al. (2019). Unified concepts for understanding and modeling turnover of dissolved organic matter from freshwaters to the ocean: The UniDOM model. *Biogeochemistry*, 146(2), 105–123. https://doi.org/10.1007/s10533-019-00621-1
- Andrews, E. D., & Antweiler, R. C. (2012). Sediment fluxes from California coastal rivers: The influences of climate, geology, and topography. The Journal of Geology, 120(4), 349–366. https://doi.org/10.1086/665733
- Ausín, B., Bruni, E., Haghipour, N., Welte, C., Bernasconi, S. M., & Eglinton, T. I. (2021). Controls on the abundance, provenance, and age of organic carbon buried in continental margin sediments. Earth and Planetary Science Letters, 558, 116759. https://doi.org/10.1016/j.epsl.2021.116759
- Balco, G., Finnegan, N., Gendaszek, A., Stone, J. O., & Thompson, N. (2013). Erosional response to northward-propagating crustal thickening in the coastal ranges of the U.S. Pacific Northwest. *American Journal of Science*, 313(8), 790–806. https://doi.org/10.2475/11.2013.01
- Bandstra, L., Hales, B., & Takahashi, T. (2006). High-frequency measurements of total CO₂: Method development and first oceanographic observations. *Marine Chemistry*, 100(1–2), 24–38. https://doi.org/10.1016/j.marchem.2005.10.009
- Bao, H., Lee, T.-Y., Huang, J.-C., Feng, X., Dai, M., & Kao, S. J. (2015). Importance of Oceanian small mountainous rivers (SMRs) in global land-to-ocean output of lignin and modern biospheric carbon. *Scientific Reports*, 5(1), 16217. https://doi.org/10.1038/srep16217

Acknowledgments

The authors confirm that there a no financial or other perceived conflicts of interest with respect to the results of this paper. Funding for this work was provided to the authors by a grant (Award # 1655506) from the U.S. National Science Foundation. The authors would like to extend our thanks to Jesse Muratli, Coby Ayres, Callie Covington, Erin Guillory, Jackie Corpus, and Josef Vincent for their help in the field and laboratory. Chris Russo and Beth Rutila assisted with analvses conducted in the Keck Lab. William Fairchild, Burke Hales, and Joe Jennings helped with the HCO3 analyses. The authors thank Peter Steele for facilitating access to the Angelo Coast Reserve and Jay Harris for assistance with permitting for sampling in Humboldt Redwoods State Park. This paper benefited from review by two anonymous reviewers.

GOÑI ET AL. 26 of 30

- Basu, N. B., Thompson, S. E., & Rao, P. S. C. (2011). Hydrologic and biogeochemical functioning of intensively managed catchments: A synthesis of top-down analyses. Water Resources Research, 47(10), W00J15. https://doi.org/10.1029/2011WR010800
- Benway, H., Alin, S., Boyer, E., Cai, W.-J., Coble, P., Cross, J., et al. (2016). A science plan for carbon cycle research in North American coastal waters. In *Report of the Coastal Carbon Synthesis (CCARS) Community Workshop*, 19–21 August 2014 (p. 84). Ocean Carbon and Biogeochemistry Program and North American Carbon Program.
- Beusen, A. H. W., Dekkers, A. L. M., Bouwman, A. F., Ludwig, W., & Harrison, J. (2005). Estimation of global river transport of sediments and associated particulate C, N, and P. Global Biogeochemical Cycles, 19(4), GB4S05. https://doi.org/10.1029/2005GB002453
- Bidlack, A., Bisbing, S., Buma, B., Diefenderfer, H., Fellman, J., Floyd, W., et al. (2021). Climate-mediated changes to linked terrestrial and marine ecosystems across the Northeast Pacific coastal temperate rainforest margin. *BioScience*, 71(6), 581–595. https://doi.org/10.1093/biosci/biosl171
- Bierman, P., Clapp, E., Nichols, K., Gillespie, A., & Caffee, M. (2001). Using cosmogenic nuclide measurements in sediments to understand background rates of erosion and sediment transport. In R. S. Harmon, & W. W. DoeIII (Eds.), *Landscape erosion and evolution modeling* (pp. 89–115). Kluwer. https://doi.org/10.1007/978-1-4615-0575-4_5
- Blair, N. E., & Aller, R. C. (2012). The fate of terrestrial organic carbon in the marine environment. Annual Review of Marine Science, 4(1), 401–423. https://doi.org/10.1146/annurev-marine-120709-142717
- Bright, C. E., Mager, S. M., & Horton, S. L. (2020). Catchment-scale influences on riverine organic matter in southern New Zealand. Geomorphology, 353, 107010. https://doi.org/10.1016/j.geomorph.2019.107010
- Brown, W. M., & Ritter, J. R. (1971). Sediment transport and turbidity in the Eel River basin. U.S. Government Printing Office.
- Bywater-Reyes, S., Segura, C., & Bladon, K. D. (2017). Geology and geomorphology control suspended sediment yield and modulate increases following timber harvest in temperate headwater streams. *Journal of Hydrology*, 548, 754–769. https://doi.org/10.1016/j.jhydrol.2017.03.048
- Checkley, D. M., & Barth, J. A. (2009). Patterns and processes in the California Current System. *Progress in Oceanography*, 83(1–4), 49–64. https://doi.org/10.1016/j.pocean.2009.07.028
- Clark, K. E., Stallard, R. F., Murphy, S. F., Scholl, M. A., González, G., Plante, A. F., & McDowell, W. H. (2022). Extreme rainstorms drive exceptional organic carbon export from forested humid-tropical rivers in Puerto Rico. Nature Communications, 13(1), 2058. https://doi.org/10.1038/s41467-022-29618-5
- Clarke, S. H. (1992). Geology of the Eel River Basin and adjacent region: Implications for Late Cenozoic tectonics of the Southern Cascadia subduction zone and Mendocino triple junction. The American Association of Petroleum Geologists Bulletin, 76, 199–224.
- Cohn, T. A., Caulder, D. L., Gilroy, E. J., Zynjuk, L. D., & Summers, R. M. (1992). The validity of a simple statistical model for estimating fluvial constituent loads—An empirical study involving nutrient loads entering Cheaseapeake Bay. Water Resources Research, 28(9), 2353–2363. https://doi.org/10.1029/92wr01008
- Cohn, T. A., DeLong, L. L., Gilroy, E. J., Hirsch, R. M., & Wells, D. K. (1989). Estimating constituent loads. Water Resources Research, 25(5), 937–942. https://doi.org/10.1029/wr025i005p00937
- Cole, J. J., Prairie, Y. T., Caraco, N. F., McDowell, W. H., Tranvik, L. J., Striegl, R. G., et al. (2007). Plumbing the global carbon cycle: Integrating inland waters into the terrestrial carbon budget. *Ecosystems*, 10(1), 172–185. https://doi.org/10.1007/s10021-006-9013-8
- Coynel, A., Etcheber, H., Abril, G., Maneux, E., Dumas, J., & Hurtrez, J.-E. (2005). Contribution of small mountainous rivers to particulate organic carbon input in the Bay of Biscay. *Biogeochemistry*, 74(2), 151–171. https://doi.org/10.1007/s10533-004-3362-1
- Coynel, A., Seyler, P., Etcheber, H., Meybeck, M., & Orange, D. (2006). Spatial and seasonal dynamics of total suspended sediment and organic carbon species in the Congo River. *Global Biogeochemical Cycles*, 19(4), GB4019. https://doi.org/10.1029/2004gb002335
- Creed, I. F., McKnight, D. M., Pellerin, B. A., Green, M. B., Bergamaschi, B. A., Aiken, G. R., et al. (2015). The river as a chemostat: Fresh perspectives on dissolved organic matter flowing down the river continuum. *Canadian Journal of Fisheries and Aquatic Sciences*, 72(8), 1272–1285. https://doi.org/10.1139/cjfas-2014-0400
- Curtiss, D. A. (1975). Sediment yields of streams in the Umpqua River Basin Oregon. U.S. Geological Survey.
- Dhillon, G. S., & Inamdar, S. (2014). Storm event patterns of particulate organic carbon (POC) for large storms and differences with dissolved organic carbon (DOC). Biogeochemistry, 118(1–3), 61–81. https://doi.org/10.1007/s10533-013-9905-6
- Drake, T. W., Raymond, P. A., & Spencer, R. G. M. (2018). Terrestrial carbon inputs to inland waters: A current synthesis of estimates and uncertainty. Limnology and Oceanography Letters, 3(3), 132–142. https://doi.org/10.1002/lol2.10055
- Fennel, K., Simone Alin, S., Barbero, L., Evans, W., Bourgeois, T., Cooley, S., et al., (2019). Carbon cycling in the North American coastal ocean: A synthesis. *Biogeosciences*, 16(6), 1281–1304. https://doi.org/10.5194/bg-16-1281-2019
- Fuller, T. K., Perg, L. A., Willenbring, J. K., & Lepper, K. (2009). Field evidence for climate-driven changes in sediment supply leading to strath terrace formation. *Geology*, 37(5), 467–470. https://doi.org/10.1130/g25487a.1
- Gaillardet, J., Dupré, B., Louvat, P., & Allègre, C. J. (1999). Global silicate weathering and CO₂ consumption rates deduced from the chemistry of large rivers. *Chemical Geology*, 159(1–4), 3–30. https://doi.org/10.1016/s0009-2541(99)00031-5
- Gaillardet, J., Rad, S., Rivé, K., Louvat, P., Gorge, C., Allègre, C. J., & Lajeunesse, E. (2011). Orography-driven chemical denudation in the Lesser Antilles: Evidence for a new feedback mechanism stabilizing atmospheric CO₂. *American Journal of Science*, 311(10), 851–894. https://doi.org/10.2475/10.2011.02
- Galy, V., Peucker-Ehrenbrink, B., & Eglinton, T. (2015). Global carbon export from the terrestrial biosphere controlled by erosion. *Nature*, 521(7551), 204–207. https://doi.org/10.1038/nature14400
- Geyer, W. R., Hill, P. S., & Kineke, G. C. (2004). The transport, transformation, and dispersal of sediment by buoyant coastal flows. Continental Shelf Research, 24(7–8), 927–949. https://doi.org/10.1016/j.csr.2004.02.006
- Geyer, W. R., Hill, P. S., Milligan, T. G., & Traykovski, P. (2000). The structure of the Eel River Plume during floods. Continental Shelf Research, 20(16), 2067–2093. https://doi.org/10.1016/s0278-4343(00)00063-7
- Ghazi, L., Goñi, M., Haley, B. A., Muratli, J. M., & Pett-Ridge, J. C. (2022). Concentration-runoff relationships of contrasting small mountainous rivers in the Pacific Northwest, USA: Insights into the weathering of rhenium relative to other weathering products. *Geochimica et Cosmo-chimica Acta*, 337, 106–122. https://doi.org/10.1016/j.gca.2022.09.03
- Giesbrecht, I. J. W., Tank, S. E., Frazer, G. W., Hood, E., Gonzalez Arriola, S. G., Butman, D. E., et al. (2022). Watershed classification predicts streamflow regime and organic carbon dynamics in the Northeast Pacific Coastal Temperate Rainforest. Global Biogeochemical Cycles, 36(2), e2021GB007047. https://doi.org/10.1029/2021GB007047
- Godsey, S. E., Hartmann, J., & Kirchner, J. W. (2019). Catchment chemostasis revisited: Water quality responds differently to variations in weather and climate. *Hydrological Processes*, 33(24), 3056–3069. https://doi.org/10.1002/hyp.13554
- Godsey, S. E., Kirchner, J. W., & Clow, D. W. (2009). Concentration-discharge relationships reflect chemostatic characteristics of U.S. catchments. Hydrological Processes: An International Journal, 23(13), 1844–1864. https://doi.org/10.1002/hyp.7315

GOŇI ET AL. 27 of 30

- Goldsmith, S. T., Harmon, R. S., Lyons, W. B., Harmon, B. A., Ogden, F. L., & Gardner, C. B. (2015). Evaluation of controls on silicate weathering in tropical mountainous rivers: Insights from the Isthmus of Panama. Geology, 43(7), 563–566. https://doi.org/10.1130/G36082.1
- Gomez, B., Baisden, W. T., & Rogers, K. M. (2010). Variable compositions of particle-bound organic carbon in steep land river systems. *Journal of Geophysical Research*, 115(F4), F04006. https://doi.org/10.1029/2010JF001713
- Goñi, M. A., Corvi, E. R., Welch, K. A., Alegria, E., Watkins-Brandt, K., & White, A. E. (2021). Wintertime particulate organic matter distributions in surface waters of the Northern California current system. Continental Shelf Research, 213, 104312. https://doi.org/10.1016/j.csr.2020.104312
- Goñi, M. A., Corvi, E. R., Welch, K. A., Buktenica, M., Lebon, K., Alleau, Y., & Juranek, L. W. (2019). Particulate organic matter distributions in surface waters of the Pacific Arctic shelf during the late summer and fall season. *Marine Chemistry*, 211, 75–93. https://doi.org/10.1016/j.
- Goni, M. A., Ghazi, L., Pett-Ridge, J., Haley, B., & Welch, K. A. (2022). Particulate and dissolved solids and organic carbon concentration data in Eel and Umpqua Rivers. HydroShare. Retrieved from http://www.hydroshare.org/resource/541f700185ed460ab0fa719b99e40ee4
- Goñi, M. A., Hatten, J. A., Wheatcroft, R. A., & Borgeld, J. (2013). Particulate organic matter export by two contrasting small mountainous rivers in the Pacific Northwest, U.S.A. *Journal of Geophysical Research—Biogeosciences*, 118(1), 112–134. https://doi.org/10.1002/jgrg.20024
- Goñi, M. A., Lerczak, J. A., Smith, L., Lemagie, E. P., & Alleau, Y. (2014). Seasonal and event scale forcings on the magnitude and composition of particulate organic matter fluxes across a small Mountainous River estuary. American Geophysical Union. Fall Meeting 2014, abstract id. B431-04
- Gray, A. B., Pasternack, G. B., Watson, E. B., & Goñi, M. A. (2016). Abandoned channel fill sequences in the tidal estuary of a small mountainous, dry-summer river. Sedimentology, 63(1), 176–206. https://doi.org/10.1111/sed.12223
- Gulick, S. P. S., Meltzer, A. S., & Clarke, S. H. (2002). Effect of the northward-migrating Mendocino triple junction on the Eel River forearc basin, California: Stratigraphic development. *Geological Society of America Bulletin*, 114(2), 178–191. https://doi.org/10.1130/0016-7606(2002)114<0178:eotnmm>2.0.co;2
- Hastings, R. H., Goñi, M. A., Wheatcroft, R. A., & Borgeld, J. (2012). A terrestrial organic matter depocenter on a high-energy margin: The Umpqua River system, Oregon. Continental Shelf Research, 39–40, 78–91. https://doi.org/10.1016/j.csr.2012.04.002
- Hatten, J. A., Goñi, M. A., & Wheatcroft, R. A. (2012). Chemical characteristics of particulate organic matter from a small mountainous river in the Oregon Coast Range, USA. *Biogeochemistry*, 107(1–3), 43–66. https://doi.org/10.1007/s10533-010-9529-z
- Heimsath, A. M., Dietrich, W. E., Nishiizumi, K., & Finkel, R. C. (2001). Stochastic processes of soil production and transport: Erosion rates, topographic variation and cosmogenic nuclides in the Oregon Coast Range. Earth Surface Processes and Landforms, 26(5), 531–552. https://doi.org/10.1002/esp.209
- Henderikx Freitas, F., Saldías, G. S., Goñi, M., Shearman, R. K., & White, A. E. (2018). Temporal and spatial dynamics of physical and biological properties along the Endurance Array of the California Current ecosystem. *Oceanography*, 31(1), 80–89. https://doi.org/10.5670/oceanog.2018.113
- Hilton, R. G., & West, A. J. (2020). Mountains, erosion, and the carbon cycle. Nature Reviews Earth & Environment, 1(6), 284–299. https://doi.org/10.1038/s43017-020-0058-6
- Hood, E., Fellman, J. B., & Spencer, R. G. M. (2020). Glacier loss impacts riverine organic carbon transport to the ocean. Geophysical Research Letters, 47(19), e2020GL089804. https://doi.org/10.1029/2020GL089804
- Janda, R. J., & Nolan, K. M. (1979). Stream sediment discharge in northwestern California. In Guidebook to a field trip to observe natural and management-related erosion in Franciscan terrane of Northern California (Vol. IV, pp. 1–27). Geological Society of America Cordilleran Section
- Karlin, R. (1980). Sediment sources and clay mineral distributions off the Oregon coast. Journal of Sedimentary Research, 50(2), 543-559.
- Kaushal, S. S., Gold, A. J., Bernal, S., Newcomer Johnson, T. A., Addy, K., Burgin, A., et al. (2018). Watershed "chemical cocktails": Forming novel elemental combinations in anthropocene fresh waters. *Biogeochemistry*, 141(3), 281–305. https://doi.org/10.1007/s10533-018-0502-6
- Kelsey, H. M. (1977). Landsliding, channel changes, sediment yield and land use in the Van Duzen River basin, north coastal California, 1941–1975 (Ph.D. thesis). University of California.
- Kelsey, H. M. (1980). A sediment budget and an analysis of geomorphic process in the Van Duzen River basin, north coastal California, 1941–1975: Summary. Geological Society of America Bulletin, 91(4), 190–195. https://doi.org/10.1130/0016-7606(1980)91<190:asbaaa>2.0.co;2
- Kelsey, H. M., Ticknor, R. L., Bockheim, J. G., & Mitchell, C. E. (1996). Quaternary upper plate deformation in coastal Oregon. Geological Society of America Bulletin, 108(7), 843–860. https://doi.org/10.1130/0016-7606(1996)108<0843:qupdic>2.3.co;2
- Kieft, B., Crump, B., White, A. E., Goñi, M. A., & Mueller, R. S. (2020). Winter river plumes shape community composition and activity of heterotrophic microorganisms on the Oregon Coast. Aquatic Microbial Ecology, 84(1), 15–29. https://doi.org/10.3354/ame01922
- Kieft, B., Li, Z., Bryson, S., Crump, B. C., Hettich, R., Pan, C., et al. (2018). Microbial community structure—Function relationships in Yaquina Bay Estuary reveal spatially distinct carbon and nitrogen cycling capacities. Frontiers in Microbiology, 9, 1282. https://doi.org/10.3389/ fmicb.2018.012829
- Kniskern, T. A., Warrick, J. A., Farnsworth, K. L., Wheatcroft, R. A., & Goñi, M. A. (2011). Coherence of river and ocean conditions along the U.S. West Coast during storms. *Continental Shelf Research*, 31(7–8), 789–805. https://doi.org/10.1016/j.csr.2011.01.012
- Kolesnichenko, I., Kolesnichenko, L. G., Vorobyev, S. N., Shirokova, L. S., Semiletov, I. P., Dudarev, O. V., et al. (2021). Landscape, soil, lithology, climate and permafrost control on dissolved carbon, major and trace elements in the Ob River, Western Siberia. Water, 13(22), 3189. https://doi.org/10.3390/w13223189
- Laraque, A., Castellanos, B., Steiger, J., Lopez, J. L., Pandi, A., Rodriguez, M., et al. (2013). A comparison of the suspended and dissolved matter dynamics of two large inter-tropical rivers draining into the Atlantic Ocean: The Congo and the Orinoco. *Hydrological Processes*, 27(15), 2153–2170. https://doi.org/10.1002/hyp.9776
- Leithold, E. L., Blair, N. E., & Perkey, D. W. (2006). Geomorphologic controls on the age of particulate organic carbon from small mountainous and upland rivers. *Global Biogeochemical Cycles*, 20(3), GB3022. https://doi.org/10.1029/2005GB002677
- Leithold, E. L., & Hope, R. S. (1999). Deposition and modification of a flood layer on the Northern California shelf: Lessons from and about the fate of terrestrial particulate organic carbon. *Marine Geology*, 154(1–4), 183–195. https://doi.org/10.1016/s0025-3227(98)00112-1
- Lin, B., Liu, Z., Eglinton, T. I., Kandasamy, S., Blattmann, T. M., Haghipour, N., et al. (2020). Island-wide variation in provenance of riverine sedimentary organic carbon: A case study from Taiwan. Earth and Planetary Science Letters, 539, 116238. https://doi.org/10.1016/j.epsl.2020.116238
- Lloret, E., Dessert, C., Pastor, L., Lajeunesse, E., Crispi, O., Gaillardet, J., & Benedetti, M. F. (2013). Dynamic of particulate and dissolved organic carbon in small volcanic mountainous tropical watersheds. Chemical Geology, 351, 229–244. https://doi.org/10.1016/j.chemgeo.2013.05.023
 Ludwig, W., Probst, J. L., & Kempe, S. (1996). Predicting the oceanic input of organic carbon by continental erosion. Global Biogeochemical
- Cycles, 10(1), 23–41. https://doi.org/10.1029/95gb02925

GOÑI ET AL. 28 of 30

- Malara, G., Zema, D. M., Arena, F., Bombino, G., & Zimbone, S. M. (2020). Coupling watershed—Coast systems to study evolutionary trends: A review. Earth-Science Reviews, 201, 103040. https://doi.org/10.1016/j.earscirev.2019.103040
- Marshall, J. A., Roering, J. J., Gavin, D. G., & Granger, D. E. (2017). Late Quaternary climatic controls on erosion rates and geomorphic processes in western Oregon, USA. GSA Bulletin, 129(5–6), 715–731. https://doi.org/10.1130/B31509.1
- Mazzini, P. L. F., Barth, J. A., Shearman, R. K., & Erofeev, A. (2014). Buoyancy-driven coastal currents off Oregon during fall and winter. *Journal of Physical Oceanography*, 44(11), 2854–2876. https://doi.org/10.1175/jpo-d-14-0012.1
- Meybeck, M., Laroche, L., Durr, H. H., & Syvitski, J. P. M. (2003). Global variability of daily total suspended solids and their fluxes in rivers. Global and Planetary Change, 39(1–2), 65–93. https://doi.org/10.1016/S0921-8181(03)00018-3
- Milliman, J. D., & Farnsworth, K. L. (2013). River discharge to the coastal ocean: A global synthesis. Cambridge University Press.
- Milliman, J. D., & Syvitski, J. P. M. (1992). Geomorphic/tectonic control of sediment discharge to the ocean: The importance of small mountainous rivers. *The Journal of Geology*, 100(5), 525–544. https://doi.org/10.1086/629606
- Mitchell, C. E., Vincent, P., Weldon, R. J., & Richards, M. A. (1994). Present-day vertical deformation of the Cascadia margin, Pacific Northwest, United States. *Journal of Geophysical Research*, 99(B6), 12257–12277. https://doi.org/10.1029/94jb00279
- Moatar, F., Abbott, B. W., Minaudo, C., Curie, F., & Pinay, G. (2017). Elemental properties, hydrology, and biology interact to shape concentration-discharge curves for carbon, nutrients, sediment, and major ions. Water Resources Research, 53(2), 1270–1287. https://doi. org/10.1002/2016WR019635
- Moukandi N'kaya, G. D., Orange, D., Bayonne Padou, S. M., Datok, P., & Laraque, A. (2020). Temporal variability of sediments, dissolved solids, and dissolved organic matter fluxes in the Congo River at Brazzaville/Kinshasa. Geosciences, 10(9), 341. https://doi.org/10.3390/geosciences10090341
- Musolff, A., Schmidt, C., Selle, B., & Fleckenstein, J. H. (2015). Catchment controls on solute export. Advances in Water Resources, 86, 133–146. https://doi.org/10.1016/j.advwatres.2015.09.026
- Omernik, J. M. (1987). Ecoregions of the conterminous United States. Map (scale 1:7,500,000). Annals of the Association of American Geographers, 77(1), 118–125. https://doi.org/10.1111/j.1467-8306.1987.tb00149.x
- Peck, E. K., Wheatcroft, R. A., & Brophy, L. S. (2020). Controls on sediment accretion and blue carbon burial in tidal saline wetlands: Insights from the Oregon coast, USA. *Journal of Geophysical Research: Biogeosciences*, 125(2), e2019JG005464. https://doi.org/10.1029/2019JG005464
- Pullen, J., & Allen, J. S. (2001). Modeling studies of the coastal circulation off Northern California: Statistics and patterns of wintertime flow. Journal of Geophysical Research, 106(C11), 26959–26984. https://doi.org/10.1029/2000jc000548
- Raymond, P. A., & Saiers, J. (2010). Event controlled DOC export from forested watersheds. Biogeochemistry, 100(1), 197–209. https://doi.org/10.1007/s10533-010-9416-7
- Raymond, P. A., Saiers, J. E., & Sobczak, W. V. (2016). Hydrological and biogeochemical controls on watershed dissolved organic matter transport: Pulse-shunt concept. *Ecology*, 97(1), 5–16. https://doi.org/10.1890/14-1684.1
- Reddy, S. K. K., Guptab, H., & Reddy, D. V. (2019). Dissolved inorganic carbon export by mountainous tropical rivers of the Western Ghats, India. *Chemical Geology*, 530, 119316. https://doi.org/10.1016/j.chemgeo.2019.119316
- Saldías, G. S., Strub, P. T., & Shearman, R. K. (2020). Spatio-temporal variability and ENSO modulation of turbid freshwater plumes along the Oregon coast. Estuarine, Coastal, and Shelf Science, 243, 106880. https://doi.org/10.1016/j.ecss.2020.106880
- Shanley, J. B., McDowell, W. H., & Stallard, R. F. (2011). Long-term patterns and short-term dynamics of stream solutes and suspended sediment in a rapidly weathering tropical watershed. Water Resources Research, 47(7), W07515. https://doi.org/10.1029/2010WR009788
- Syvitski, J. P. M., & Kettner, K., (2011). Sediment flux and the anthropocene. *Philosophical Transactions of the Royal Society A*, 369(1938), 957–975, https://doi.org/10.1098/rsta.2010.0329
- Syvitski, J. P. M., Morehead, M. D., Bahr, D. B., & Mulder, T. (2000). Estimating fluvial sediment transport: The rating parameters. Water Resources Research, 36(9), 2747–2760. https://doi.org/10.1029/2000wr900133
- Syvitski, J. P. M., Peckham, S. D., Hilberman, R. D., & Mulder, T. (2003). Predicting the terrestrial flux of sediment to the global ocean: A planetary perspective. Sedimentary Geology, 162(1–2), 5–24. https://doi.org/10.1016/s0037-0738(03)00232-x
- Thompson, S. E., Basu, N. B., Lascurain, J., Jr., Aubeneau, A., & Rao, P. S. C. (2011). Relative dominance of hydrologic versus biogeochemical factors on solute export across impact gradients. *Water Resources Research*, 47(10). https://doi.org/10.1029/2010wr009605
- Thomsen, L., Aguzzi, J., Costa, C., De Leo, F., Ogston, A., & Purser, A. (2017). The oceanic biological pump: Rapid carbon transfer to depth at continental margins during winter. *Scientific Reports*, 7(1), 10763. https://doi.org/10.1038/s41598-017-11075-6
- Thurman, E. M. (1985). Organic geochemistry of natural waters (developments in biogeochemistry) (p. 497). Martinus NijHoff/DR W. Junk Publishers. https://doi.org/10.1007/978-94-009-5095-5
- Torres, M. A., West, A. J., & Clark, K. E. (2015). Geomorphic regime modulates hydrologic control of chemical weathering in the Andes-Amazon. Geochimica et Cosmochimica Acta, 166, 105–128. https://doi.org/10.1016/j.gca.2015.06.007
- Walsh, J. P., & Nittrouer, C. A. (2009). Understanding fine-grained river-sediment dispersal on continental margins. *Marine Geology*, 263(1–4), 34–45. https://doi.org/10.1016/j.margeo.2009.03.016
- Ward, N. D., Bianchi, T. S., Medeiros, P. M., Seidel, M., Richey, J. E., Keil, R. G., & Sawakuchi, H. O. (2017). Where carbon goes when water flows: Carbon cycling across the aquatic continuum. *Frontiers in Marine Science*, 4, 7. https://doi.org/10.3389/fmars.2017.00007
- Wetz, M. S., Hales, B., Chase, Z., Wheeler, P. A., & Whitney, M. M. (2006). Riverine input of macronutrients, iron, and organic matter to the coastal ocean off Oregon, USA, during the winter. *Limnology & Oceanography*, 51(5), 2221–2231. https://doi.org/10.4319/lo.2006.51.5.2221
- Wheatcroft, R. A. (2000). Oceanic flood sedimentation: A new perspective. Continental Shelf Research, 20(16), 2059–2066. https://doi.org/10.1016/s0278-4343(00)00062-5
- Wheatcroft, R. A., & Borgeld, J. C. (2000). Oceanic flood layers on the Northern California margin: Large-scale distribution and small-scale physical properties. *Continental Shelf Research*, 20(16), 2163–2190. https://doi.org/10.1016/s0278-4343(00)00066-2
- Wheatcroft, R. A., Goñi, M. A., Hatten, J. A., Pasternack, G. B., & Warrick, J. A. (2010). The role of effective discharge in the ocean delivery of particulate organic carbon by small, mountainous river systems. *Limnology & Oceanography*, 55(1), 161–171. https://doi.org/10.4319/10.2010.55.1.0161
- Wheatcroft, R. A., Goñi, M. A., Richardson, K. N., & Borgeld, J. C. (2013). Natural and human impacts on centennial sediment accumulation patterns on the Umpqua River margin, Oregon. *Marine Geology*, 339, 44–56. https://doi.org/10.1016/j.margeo.2013.04.015
- Wheatcroft, R. A., & Sommerfield, C. K. (2005). River sediment flux and shelf sediment accumulation rates on the Pacific Northwest margin. Continental Shelf Research, 25(3), 311–332. https://doi.org/10.1016/j.csr.2004.10.001
- Willenbring, J. K., Gasparini, N. M., Crosby, B. T., & Brocard, G. (2013). What does a mean? The temporal evolution of detrital cosmogenic denudation rates in a transient landscape. *Geology*, 41(12), 1215–1218. https://doi.org/10.1130/g34746.1
- Wise, D. R., & O'Connor, J. (2016). A spatially explicit suspended-sediment load model for Western Oregon (No. 2016-5079). U.S. Geological Survey.

GOŇI ET AL. 29 of 30



Journal of Geophysical Research: Biogeosciences

10.1029/2022JG007084

Zarnetske, J. P., Bouda, M., Abbott, B. W., Saiers, J., & Raymond, P. A. (2018). Generality of hydrologic transport limitation of watershed organic carbon flux across ecoregions of the United States. *Geophysical Research Letters*, 45(21), 11702–11711. https://doi.org/10.1029/2018GL080005 Zhao, B., Yao, P., Bianchi, T. S., & Yu, Z. G. (2021). Controls on organic carbon burial in the Eastern China Marginal Seas: A regional synthesis. *Global Biogeochemical Cycles*, 35(4), e2020GB006608. https://doi.org/10.1029/2020GB006608

Zitoun, R., Achterberg, E. P., Browning, T. J., Hoffmann, L. J., Krisch, S., Sander, S. G., & Koschinsky, A. (2021). The complex provenance of Cu-binding ligands in the South-East Atlantic. *Marine Chemistry*, 237, 104047. https://doi.org/10.1016/j.marchem.2021.104047

GOÑI ET AL. 30 of 30